Moors for the Future Small Project Grant

No A79419_spg_Man_McMorrow

Final report, July 2006

Mapping and encoding the spatial pattern of peat erosion

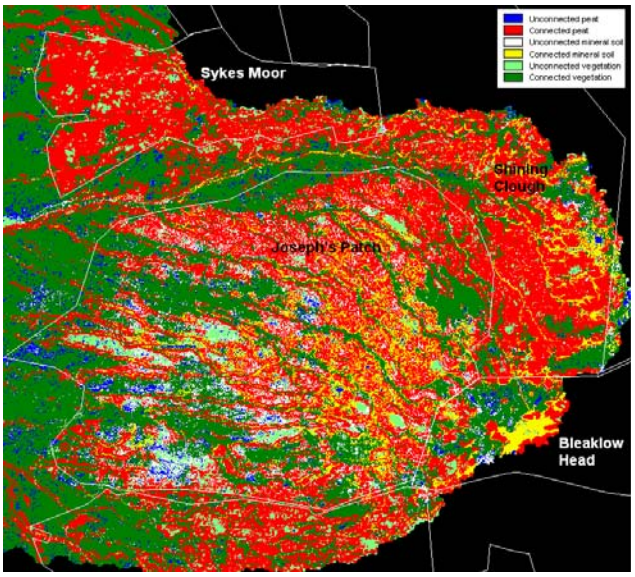

Julia McMorrow

John Lindsay

Laura Liddaman

julia.mcmorrow@manchester.ac.uk

Upland Environments Research Unit, Geography,
School of Environment and Development, The University of Manchester,
Manchester M13 9PL

CONTENTS

LIST OF FIGURES

LIST OF TABLES

1. INTRODUCTION

1.1 Context

Blanket peat covers approximately 300 km^2 of the southern Pennines, and three quarters has been badly affected by erosion (Bragg and Tallis, 2001). Degraded peatland landscapes are a mosaic of exposed peat, mineral soil and vegetation patches. The size, shape, arrangement and topographic association of the peat and mineral soil patches produce patterns which express the erosion status of the catchment.

The most degraded catchments of the Dark Peak are characterised by large areas of exposed peat and mineral soil. Vegetation cover has been lost and gully erosion has proceeded down through the peat to underlying mineral soil, followed by lateral erosion to produce mineral-floored gullies and, eventually, large expanses of mineral soil with isolated mounds of bare peat, as at Bleaklow Head. Export of particulate organic carbon (POC) in streamflow is greater from degraded catchments, with consequent siltation in reservoirs (Evans and Warburton, 2005). High levels of dissolved organic carbon (DOC) are also present in the streams, darkening water colour in reservoirs (Freeman *et al*., 2001; Labadz *et al.,* 1991). Export of POC and DOC in streamflow and aerobic decomposition from exposed peat flats represent losses in the peatland carbon cycle and its contribution to the overall carbon budget (Stewart and Wheatly, 1990; Gorham, 1991; Charman, 2002; Worrall *et al*., 2003; Holden, 2005).

For POC, it is not simply the area of exposed peat and mineral soil which is important; so too is the arrangement of pat patches in the landscape. The underlying premise is that pattern is a proxy for process (Belyea and Lancaster 2002). Specifically, it can be suggested that the connectivity of peat patches to channels is an indicator of erosion risk, expressing slope-channel coupling in bare peat areas. It is a major control on sediment export because vegetation patches connected to channels act as sediment traps (Evans *et al*., in press). Thus, if we can encode patch-channel connectivity[1] and other key elements of erosion pattern, we could use these pattern metrics to classify peat patches and map the potential for loss of POC in peatland catchments (Liddaman, 2004; Liddaman *et al*., 2004). Patches where restoration works would be likely to produce the greatest reduction in POC could be identified, that is, where connectivity to channels is highest and where metrics such as area and slope suggest that risk is highest.

The project evaluates alternative techniques and existing aerial photography datasets for mapping peat erosion for two contrasting sample catchments, and develops a method for encoding the erosion pattern. By extending the method over the Peak District National Park (PDNP), priority areas for erosion control measures may be identified.

1.2 Aims

The project aim was to develop an objective, repeatable method of describing the erosion pattern, which could be used to produce a baseline map of peat erosion pattern and erosion status. It had to be based on easily accessible remotely sensed data sources. The aims were:

[1] As distinct from patch-to-patch connectivity used in landscape ecology and habitat analysis (Clergeau and Burel, 1997).

- To use existing remotely sensed datasets to provide a baseline map of peat erosion for two contrasting catchments
- To develop a technique for extracting a set of erosion pattern metrics from the baseline map, so as to provide an objective, repeatable description of peat erosion pattern

A longer term aim, beyond the scope of the current project, is to use the erosion pattern metrics to classify catchments into erosion status classes and test the extent to which they relate to relative loss of POC.

1.3 Research questions

1. What is the best existing spatial data source and method to produce a baseline (pre-restoration) map of exposed peat and mineral soil?
2. What is the most appropriate method to extract the channel network from a LiDAR digital elevation model (DEM) in eroding peatland?
3. How can we use the erosion map, channel network and digital terrain model (DTM) to derive erosion pattern metrics (*i.e.* variables which objectively describe erosion pattern within and between catchments) and to produce a map of potential erosion risk?
4. To what extent can these techniques be used to monitor the success of restoration measures over time?

1.4 Objectives

1. To evaluate the quality of available aerial photographs and recommend which should be used for mapping and encoding erosion pattern.
2. To produce a baseline three class ***map of peat erosion*** (exposed peat, mineral soil, vegetation)
3. To recommend the most appropriate classification methods.
4. To use the peat erosion map to extract ***morphological metrics*** expressing the size, and shape of peat and mineral soil patches, and, together with the DTM, to extract ***topographic metrics*** expressing their erosion potential.
5. To extract a realistic ***channel network*** from the LiDAR DTM and, together with the peat erosion map, to extract ***connectivity metrics*** describing the degree of slope-channel coupling in areas of exposed peat.
6. To use the erosion pattern metrics to illustrate and analyse ***spatial variation in erosion pattern metrics*** within and between sample catchments.
7. To derive preliminary maps of potential erosion risk based on key land cover, connectivity, morphological and topographic metrics.
8. To make recommendations for further work.

1.5 Study sites

Two catchments were selected in the Dark Peak area of the southern Pennines (Figure 1.1), near to the Snake Pass (A57) between Manchester and Sheffield, with differing proportions and patterns of exposed peat and mineral soil. They represent the range of degradation from the highly degraded at Torside (TS) to less degraded at Upper North Grain (UNG). Torside Clough is the larger of the two catchments (3.31 sq km) and has both Bower Type 1 and Type 2 erosion patterns present (Bower, 1960, 1961). Upper North Grain (UNG) (0.38 sq km) is characterised by Bower Type 1 erosion with deep incised gullies.

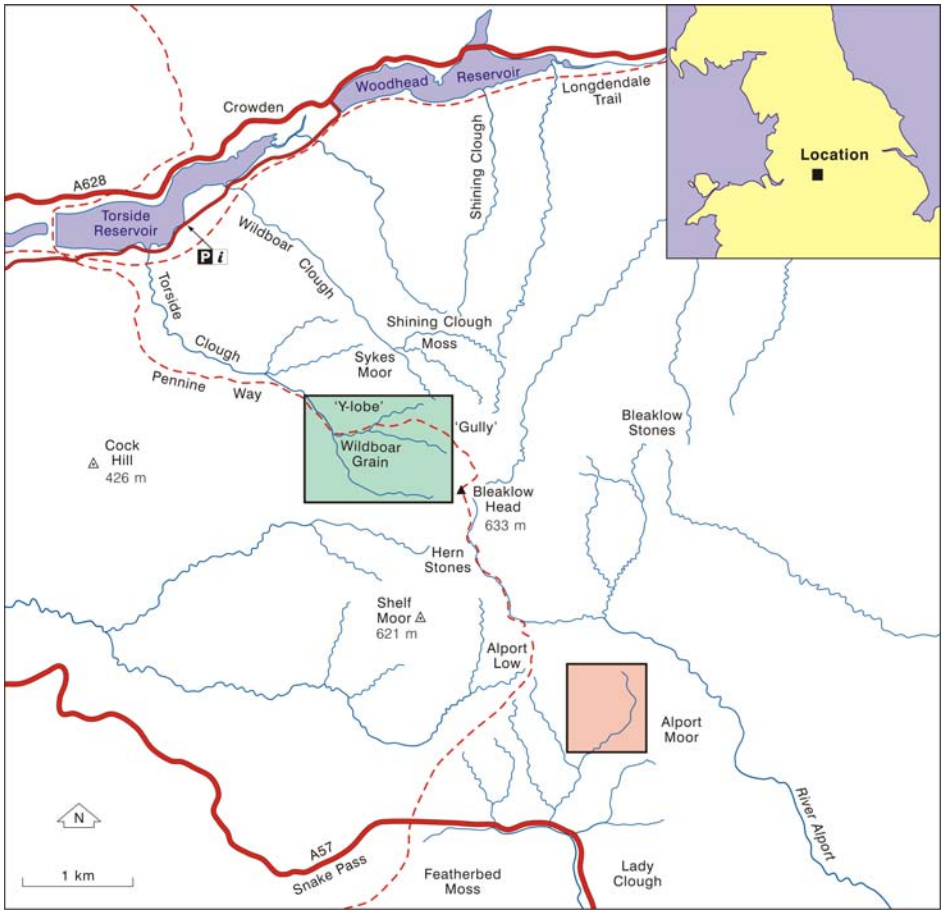

Figure 1.1: Location of Dark Peak catchments: green box, Torside (TS), red box, Upper North Grain (UNG)

1.6 Structure of report

Figure 1.2 shows the key stages in the project, which are mirrored in the report structure.

Section 2 evaluates the radiometric and geometric quality of spatial data sets available and makes preliminary recommendations about appropriate aerial photographs and DEMs for pattern work (objective 1). Brief recommendations will also made about types of remotely sensed data and classification methods which could be used to monitor revegetation resulting from moorland restoration.

Section 3 evaluates multispectral classification methods to produce the three class map of peat erosion (objectives 2 and 3) and selects the data source to be used to encode pattern (objective 1).

Section 4 explains the metrics used to pattern encode, including how pixels on the three class map are sieved and clumped to produce a patch map. It describes how morphological and topographic metrics were extracted from the patch map and digital elevation model (DEM) (objective 4). It describes a new method to extract the channel network is how patch connectivity is encoded (objective 5).

Section 5 presents a statistical analysis of how pattern metrics vary between and within catchments (objective 6) and develops preliminary erosion risk maps (objective 7).

Section 6 summaries recommendations, reflects on the degree to which aims were met and makes recommendations for further work (objective 8).

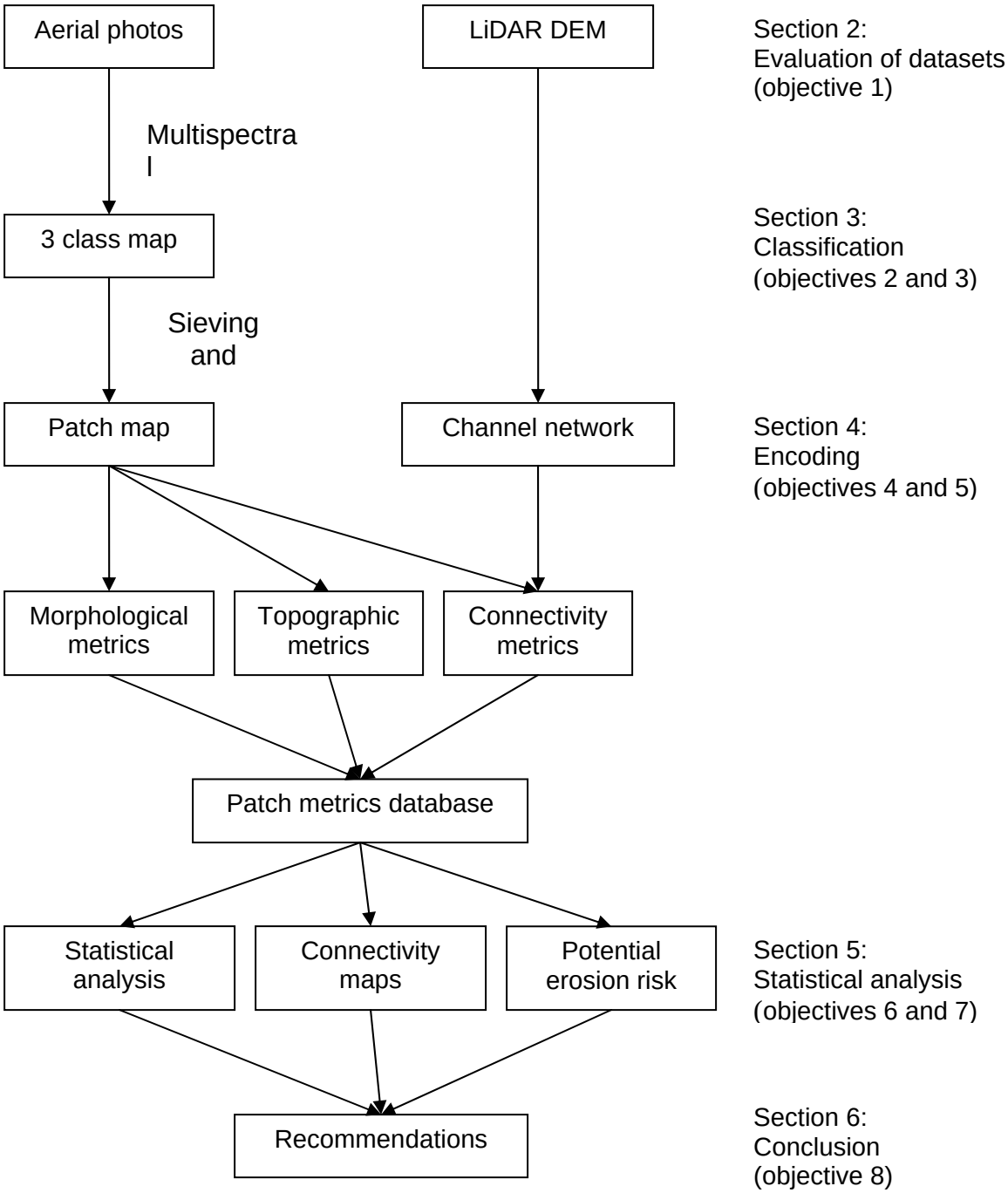

Figure 1.2: Flowchart of project work scheme and relationship to report structure

2. SPATIAL DATA SETS

2.1 LiDAR

A digital elevation model (DEM) was made available by the National Trust and MFF. A DEM is an image of the height of the land. It was needed to extract topographic metrics such as slope for the peat, mineral soil and vegetation patches, and to generate a channel network (section 4.1.2).

The DEM provided had been extracted from LiDAR data secured by the Environment Agency on two dates; 5 December 2002 for UNG (The National Trust High Peak Estate dataset) and for May 2004 for Torside (MFF extended 'Holden' data set). The 10 m pixel size of the Infoterra digital terrain model was too coarse to use with aerial photographs of 0.25 and 0.5m pixel size. A digital elevation model (DEM) is normally available as a by-product of the aerial photography orthorectification process (as for two of the three aerial photo datasets). These were produced for two of the aerial photograph datasets, UK Perspectives true colour, 1997-2001 (UKP-TC), and the UK Perspectives colour infrared, 2005 (UKP-CIR) however, they were not supplied for the project (Table 2.1). Given the extra data volume and work already undertaken on extracting a channel network from the LiDAR DEM, it was felt that the project should continue with the LiDAR.

LiDAR is an airborne laser scanner which measures the elevation of the land surface, for this dataset, every 2 m laterally and with a stated vertical accuracy of 0.10 m (Haycock, 2004). The forward motion of the aircraft builds up the lines of the image. The sensor measures the time taken for the laser pulses to return to the sensor, which is proportional to the distance between the sensor and the ground, that is, to the height of the land. The time taken for the first pulse to return gives a digital surface model (DSM), which can include buildings or tree tops. In an open moorland environment, there are few such obstacles so the DSM approximates to the ground surface itself (known strictly as a digital terrain model or DTM). The DEM used here was actually a DTM created by the Environment Agency from the DSM and corrected to remove small depressions.

2.2 Aerial photographs

Three sets of aerial photographs (APs) were provided by MFF (Figure 2.1, Table 2.1): (i) Get Mapping (GM) 0.25m, (ii) UK Perspective 0.25m true colour (UKP-TC) scanned aerial photographs and (iii) UK Perspective colour (near) infrared (UKP-CIR) aerial photographs at a resolution of 0.50m.

The GM (Figure 2.1(a)) was flown between April and October 1999 imagery, according to the suppliers, but a date of 2002 in given in the MFF data booklet (MFF 2005). They have been rectified to Ordnance Survey (OS) but have not been orthorectified, so geometric distortions due to topography remain, as do errors due to the quality of the OS data for moorland areas. The UKP-TC aerial photographs (Figure 2.1(b)) were flown between 1999 and 2003 and have been fully orthorectified with a stated map accuracy of ± 2 m. The UKP-CIR imagery (Figure 21(c)) was flown in 2005 and is fully orthorectified with a stated map accuracy of ± 2 m.

It is not clear if the GM and UKP-TC 1997-2001 datasets were acquired as analogue photographs with a photographic camera and the negatives scanned, or if they were acquired by a digital camera (often regarded erroneously as 'scanned' data). This indicates the need for good metadata from the suppliers and its subsequent maintenance.

Alternative image sources available for this work include satellite imagery and airborne scanners such as CASI and SWIR data (Palylyk *et al*., 1984; McMorrow and Hume, 1986; Weaver, 1987; Ward and Weaver, 1989; Poulin *et al*., 2002; Cutler *et al*, 2002; Mehner *et al.,* 2004). However, aerial photography was selected as it is a familiar and easily available image source for land mangers. The rationale was to develop techniques that utilise the data sources currently available to the people that will put them into practice.

Table 2.1: Metadata available for the aerial photograph datasets

Property	Get Mapping	UK Perspective-TC	UKP-CIR
Type	Scanned true colour	Scanned true colour	Digital and NIR (true colour also available)
Spectral range	Visible	Visible	Visible and NIR
Pixel Size	0.25m	0.25m	0.50m
Geometry	Not orthorectified but rectified using OS data	Fully orthorectified imagery with map accuracy ± 2 m	Fully orthorectified imagery with map accuracy ± 2 m
Date	Apr-Oct 1999 (supplier's data, 2002 in MFF data booklet)	1999-2003	Sept 2005
DEM produced	No	Yes	Yes

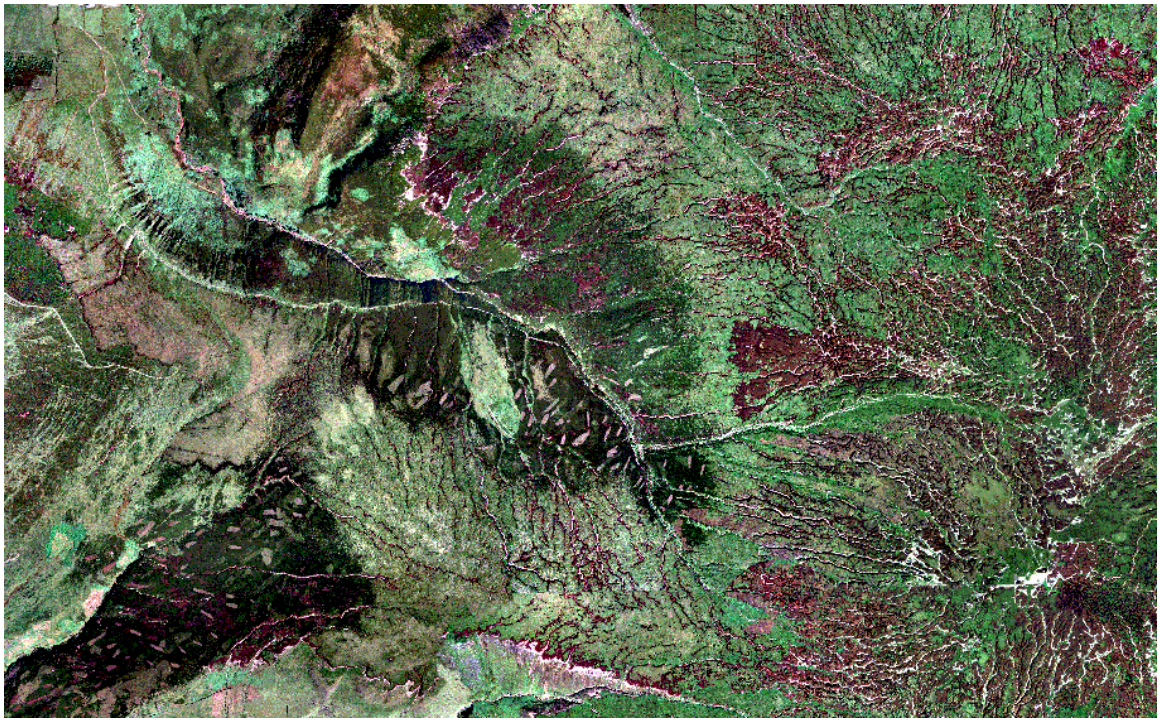

Figure 2.1(a): Extract for Torside from Get Mapping aerial photos

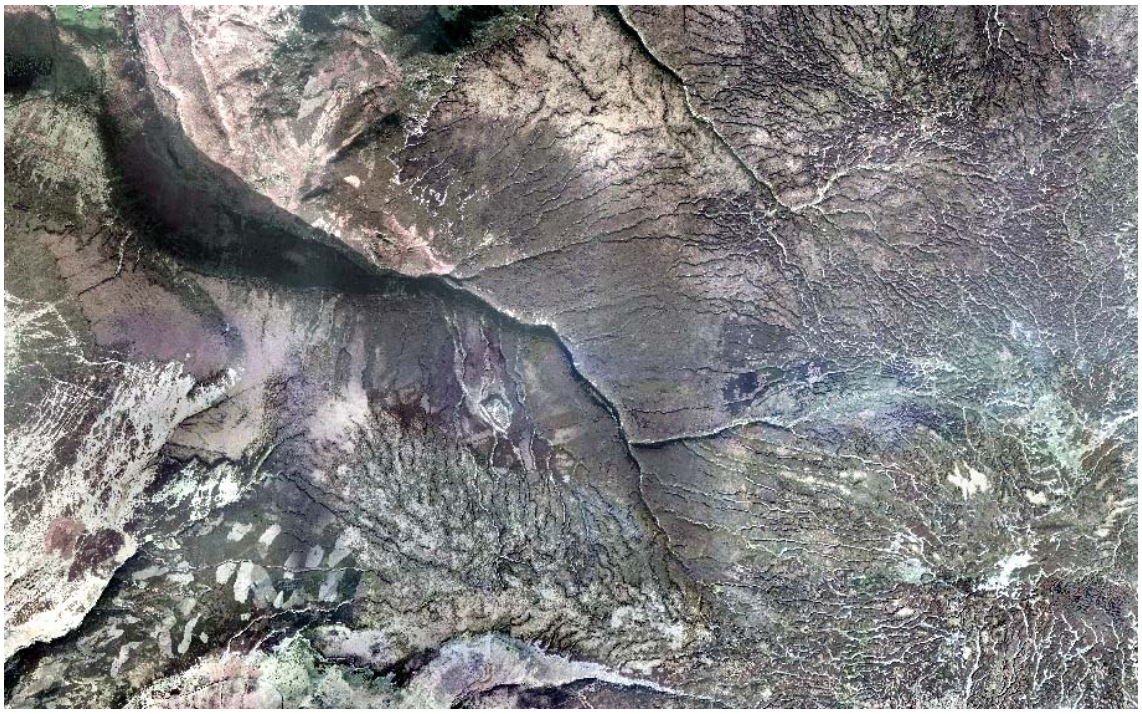

Figure 2.1(b): Extract for Torside from the UKP-TC aerial photos (1997-2001)

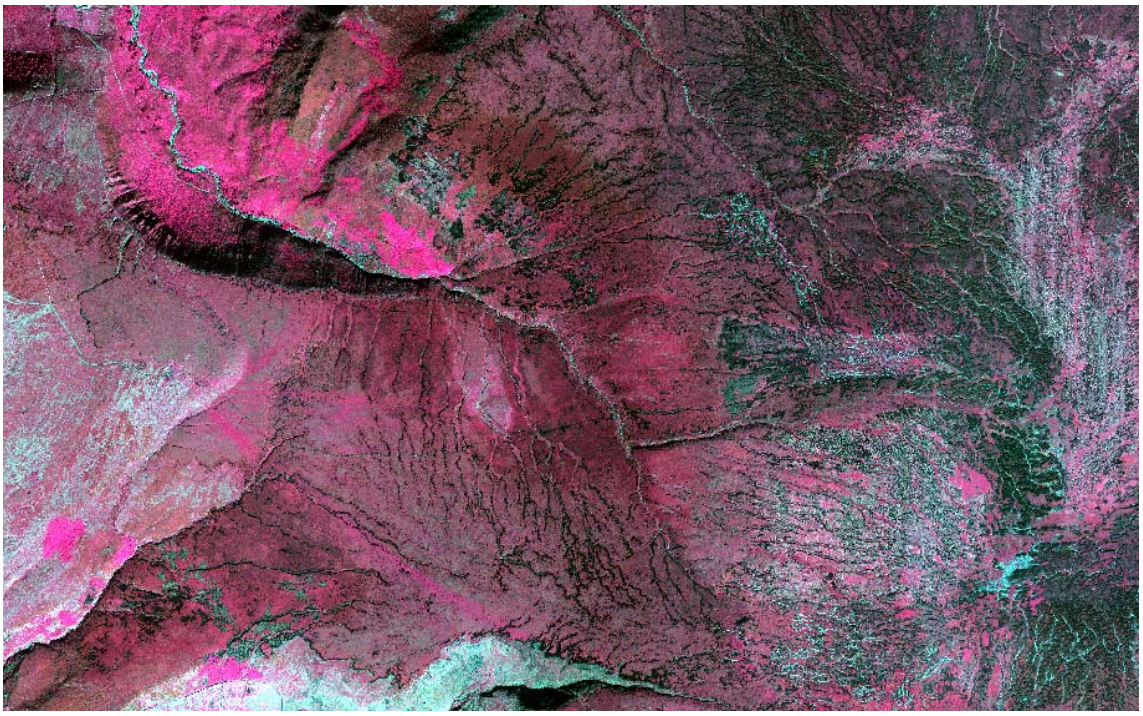

Figure 2.1(c): Extract for Torside UKP-CIR aerial photos

2.3 Assessment of aerial photo image quality

2.3.1 Rationale

A problem associated with aerial photography is that it is usually provided by external agencies and, as a result, it can be difficult to obtain full metadata, especially details of pre-processing procedures which may have been applied, such as contrast stretching, compression and geometric correction. Therefore, an assessment of the radiometric and geometric quality of the three datasets was carried out to evaluate the usefulness of the imagery for mapping and encoding the spatial pattern of peat erosion. Radiometric quality significantly affects the thematic accuracy of the patch map, that is, whether the land cover class allocated is correct. Geometric accuracy is critical to assess connectivity of peat patches to channels, since the channels derived from the LIDAR DEM must fit accurately over the patch map.

2.3.2 Method

OS mapping of sufficient accuracy is not updated frequently enough to use as the reference source; for instance, the Pennine Way has been relocated in places since OS mapping. Therefore, the LiDAR data was regarded as the base for assessing relative geometric accuracy of the aerial photography. Geometrically, the correction of the LiDAR is good as it uses two dGPS, one on board the aircraft and a second located at an OS base station whose position is known to millimetric accuracy. In this way, the position of lines can be fixed regardless of aircraft movement during scanning.

Thirty-five control points were identified on both the aerial photography and the LiDAR datasets, largely at steam confluences. This was the maximum which could be detected on all four datasets. Some could be identified on all the photographs but not on the DEM because their topography was not sufficiently pronounced at the 2m spatial resolution of the LiDAR. The root mean square error (RMSE) was calculated to express the difference in position (Table 2.2).

2.3.3 Get Mapping aerial photos

The GM imagery has good radiometric properties, although it has been heavily contrast stretched prior to Manchester University obtaining the dataset. This has enhanced spectral contrasts between the three land cover classes (exposed peat, mineral soil and vegetation), making it qualitatively and, to some extent, quantitatively possible to extract land cover information. The contrast stretch has saturated mineral soil to white, as can be seen in Figure 3.1. While this makes it easy to pick out visually (Figure 2.1(a)), it creates statistical problems for automated classification (section 3.1.3.).

The major problem with the GM imagery is that it has poor geometric accuracy because it has not been orthorectified. The RMSE relative to the LiDAR DEM was 17.49 m, which greatly reduces the usefulness of this dataset in trying to identify the connectedness of the peat patches to the channel network. As the channel network is extracted from the LiDAR data, it is important that it overlays with low positional error on the patch map (derived by classifying the APs as in section 3.1, and sieving and clumping as in section 4.1.1). If positional error is poor, then the connectivity of patches to the channel could be under or over-estimated.

2.3.4 UKP-TC aerial photos

The UKP-TC imagery had the opposite problems to the GM imagery. Geometric accuracy was significantly higher with a RMSE of 3.52 m, giving a better fit to the LiDAR data. However, radiometric properties were very poor, with poor contrast and artefacts,

including speckles and blocking (Figure 2.3). Such artefacts are usually created by file compression to reduce storage space. They produce problems if image processing, such as multispectral classification is to be carried out. It is therefore important that images are purchased in an uncompressed format, despite the extra disc space required. A 5x5 pixel median filter was applied to the UKP-TC images to reduce speckle. The filter replaces the central value in a moving window with the median brightness value for the pixels in the window (Mather, 2004).

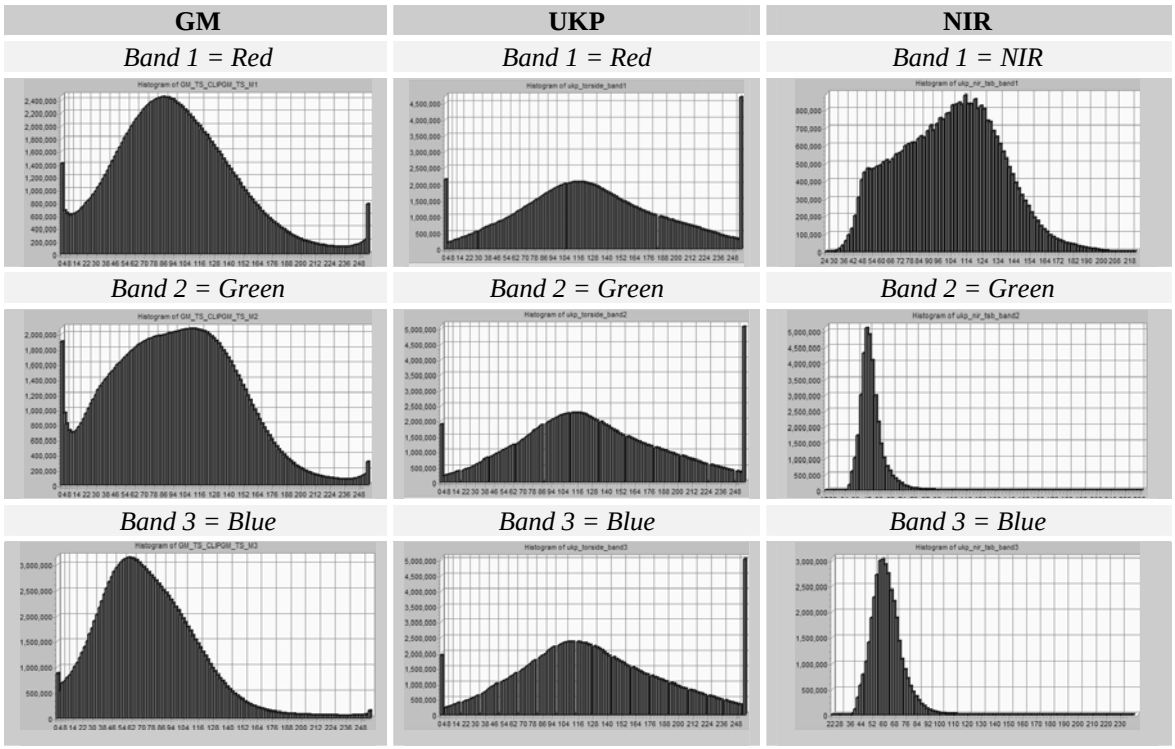

Figure 2.2: Histograms showing image brightness in three bands for the Torside image extract for each of the three aerial photo data sets.

The poor contrast of the UKP-TC photographs was confirmed by the near duplication of reflectance in two of the three image bands, as illustrated by the close similarity of their brightness histograms (Figure. 2.2), making the image look 'washed out'. This could be due to accidental duplication of a band by the distributors, or, more likely, to poor spectral contrasts between vegetation, peat and mineral soil at the season(s) the imagery was acquired. Ironically, spectral differences have probably been further reduced by the strong contrast stretch applied by the suppliers (as indicated by the small peaks at ether end of the histograms in Figure 2.2 and the saturated reflectance of mineral soil (Figure 3.1). The strong stretch may have been applied because of the great range of brightness found when many photographs are mosiacked and, especially, if they had been captured over a period of four years and at different seasons.

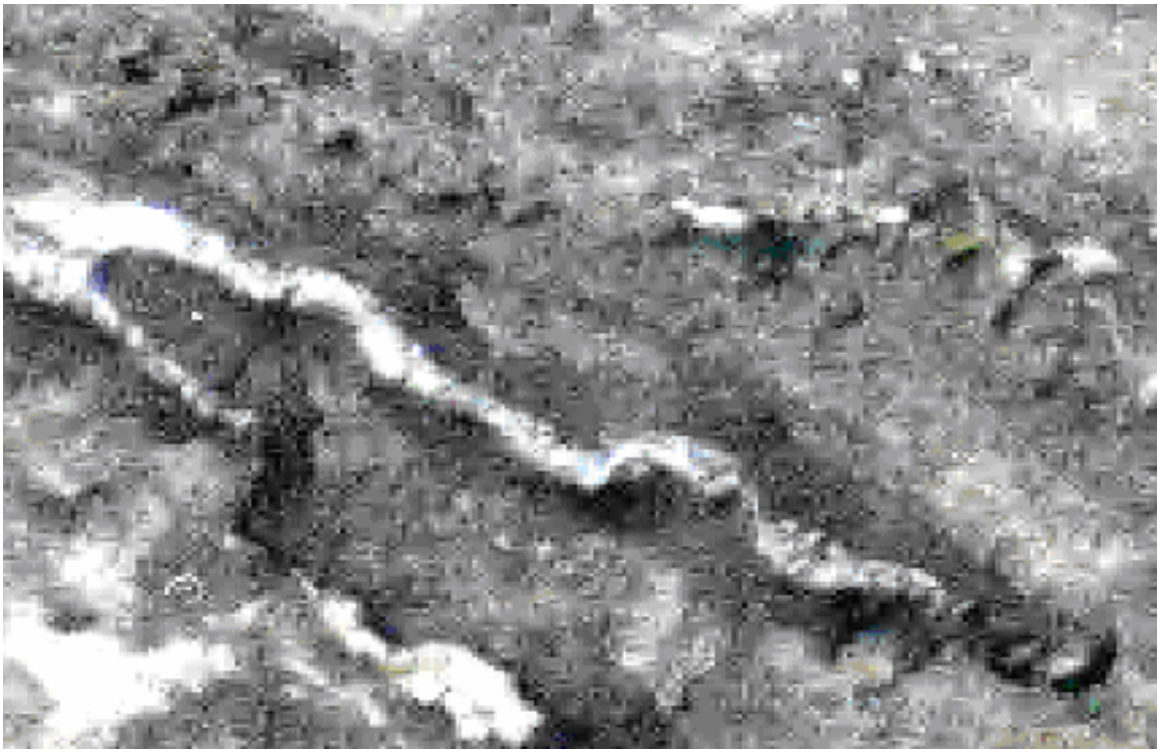

Figure 2.3: Block artefacts and speckling produced by compression in UKP true colour aerial photographs. The poor colour quality is also illustrated.

2.3.5 UKP-CIR aerial photos

The UKP-CIR imagery has the best radiometric and geometric properties of all three datasets. The NIR band separates the spectral properties of the peat and vegetation classes better, so that the UKP-CIR imagery would produce a much better map of the exposed peat, mineral soil and vegetation. However, the relatively low sun angle of these September images, seen in Figure 2.2(c), means that deeply incised areas like Torside Clough are in shadow and caused shadow to be misclassified as peat (Figure 3.5(c)). Elsewhere shadow was an advantage; it reinforced the low reflectance of peat exposed along the shaded side of gullies, especially those orientated SW-NE and helped them to be classified as peat (Figure 3.9(c)). However, the reflectance of peat on sunlit gully walls was similar to vegetation or mineral soil and caused misclassification. These issues which will be discussed in section 3.

The data were available in two formats. The 'ecw' format contained many compression artefacts which meant that it was not suitable for classification, so the 'tif' format was used instead.

The geometric properties relative to the LiDAR DEM were also excellent, with a RMSE of only 0.79m, producing a good fit with the LiDAR. The combination of good radiometric and geometric properties suggested that the UKP-CIR would produce the best peat, mineral soil vegetation map for the next stage of the analysis. This was confirmed by the assessment of thematic accuracy (section 3.4) and the classified mages UKP-CIR photos were used.

2.3 Discussion and recommendations

The quality of the imagery varies significantly for the three data sets (Table 2.2). Good radiometric and geometric quality is required for analysis of erosion pattern, and for any future monitoring of moorland restoration work. Overall the UKP-CIR photographs were found to offer the best compromise and therefore, were used to encode and statistically analyse erosion pattern (sections 4 and 5). Factors affecting patch definition are summarised in Figure 2.4.

Table 2.2: Summary of aerial photograph image quality

Properties	Get Mapping	UKP-TC	UKP-CIR
GEOMETRIC:	Very poor - Some landscape features have been distorted	Good	Very Good
RMSE *relative to LiDAR DEM*	Overall 17.49m X 8.55 Y 11.27	Overall 3.52m X 2.33 Y 1.99	Overall 0.79m X 0.96 Y 0.67
RADIOMETRIC:	Poor - heavily Stretched so does not represent the true colour of the landscape, but separates classes quite well.	Very poor – possible band replication in some areas. Stretched. Shadow. problems	Good – NIR band identifies the vegetation very well. Shadow. problems
Artefacts	None	Compression artefacts. Some white lines	None for tif format, but compression artefacts on ECW

Five recommendations can be made for any new photography commissioned:

(i) Radiometric pre-processing should be kept to a minimum, especially data should be supplied uncompressed and not contrast stretched.

If a smaller file size is also needed, data should be requested in two formats (as with the compressed 'tif' and compressed 'ecw' for UKP-CIR). Alternatively, data compression, for instance to 'jpg,' could be done in-house after delivery.

It is recommended that an archive of sub-sampled contrast stretched thumbnail images is made to make browsing easier for users, ideally referenced to a digital map of the flight plan. It is becoming easier to deliver maps and images over the internet).

Where printouts for visual interpretation are needed, contrast stretching of extracts could be done in-house using freeware such as TAS.

(ii) CIR photography is better than true colour

Including NIR part of the spectrum improves spectral separability, especially if types of vegetation or the status of revegetating peat is to be assessed. This is because plants reflect NIR light according to their leaf area, leaf structure and canopy geometry, so differences due to species composition or vigour of growth

are more detectable in this part of the spectrum (Lillesand *et al.,* 2003). Scanner images at longer wavelengths and hyperspectral images should also be explored (section 3.5).

(iii) Obtain images in summer and as close as possible to solar noon.

Timing is critical due to sun angle and plant phenology. Photography should be acquired when the high sun is high in the sky to minimise shadow, that is, summer and/or close to solar noon (12:00 GMT, 13:00 BST).

Spectral contrasts between moorland plants are most obvious in spring or summer, depending on specific habitat (McMorrow and Hume, 1986; Morton 1986). This is because seasonal changes in phenology, such as greening up or flowering, produce marked change in the reflectance of red and near infrared (NIR) light at this time, making it easier to distinguish between habitats or stages of regeneration.

(iv) Good orthorectification is required

Removal of as much geometric distortion as possible is essential for pattern analysis because patch maps must fit over the LiDAR DEM for connectivity analysis. It is also essential for locating plots established to monitor moorland restoration. Orthorectification (seeks to remove the topographic distortions to make a planimetrically accurate photomap. Rectification does not correct for topography.

It is rarely possible to remove all distortion, so it is advisable to state an acceptable RMSE (map accuracy) at the time of commissioning and to confirm that the supplier calculates RMSE from an independent set of test points and not from the control points used to carry out the orthorectification.

The source of control points and DEM to be used should also be known, as both can reduce final map accuracy. Control points fixed with a millimetric dGPS are better than those extracted from OS mapping. A DEM derived from the aerial photos themselves is preferable, followed by one from LiDAR at as fine a resolution as possible (a 2m LiDAR DEM is better than 10m).

Compromise may be needed, as reducing error incurs cost. This might be offset by requesting the DEM which is normally a by-product of ortho-rectification (unless an existing DEM is used to perform the correction). For pattern work based on the 2m LiDAR DEM, the stated map accuracy of the UKP-CIR photos, 2m, is appropriate for the DEM pixel size (the stated map accuracy of DEM not known but usually not better than ± one pixel).

The UKP-CIR photos with 0.5 m pixels and RMSE of 2 m are also appropriate for monitoring restoration at permanent 4x4 m plots. If RMSE or pixel size were larger, then larger plots would be needed to ensure that the pixels extracted relate to the ground data.

(v) Not finer than 0.5m spatial resolution unless for small areas (<1 km^2).

Data volume and cost is increased if more detailed images are used. Doubling the spatial resolution (halving pixel size) quadruples the data volume. This has implications for storing and processing files (section 4.2) unless small extracts are used. A finer resolution would not be practicable if pattern analysis were up-scaled to the whole of the Section 3 Moorlands in the National Park. Resolution issues are discussed further in the conclusion (section 6.1).

(vi) Complete metadata is required

Ideally international metadata standards should be followed. It should be updated if any changes are made after delivery. It is also helpful to have a flight plan showing photo centres. Metadata from the supplier should include:

- type of photograph (e.g. true colour, colour infrared);
- sensor, e.g. digital camera or scanned negative from an analogue photographic camera);
- date and time of acquisition for each photograph, especially where a mosaic of dates is used;
- pixel size and scan resolution in dots per inch if appropriate (for scanned prints or negatives);
- part of the spectrum for each band number of a digital file (e.g. band 1 NIR light, band 2 red light, band 3 green light);
- method of orthorectification, including software used and source of control points (e.g. dGPS, GPS, OS maps);and type of DEM used for orthorectification (e.g. OS Landform Profile 1:10,000 DTMs; NextMap, photogrammetric using previous aerial photos or those being commissioned);
- RMSE in x, y and overall, including number and source of test points;
- any radiometric pre-processing such as contrast stretching or compression.

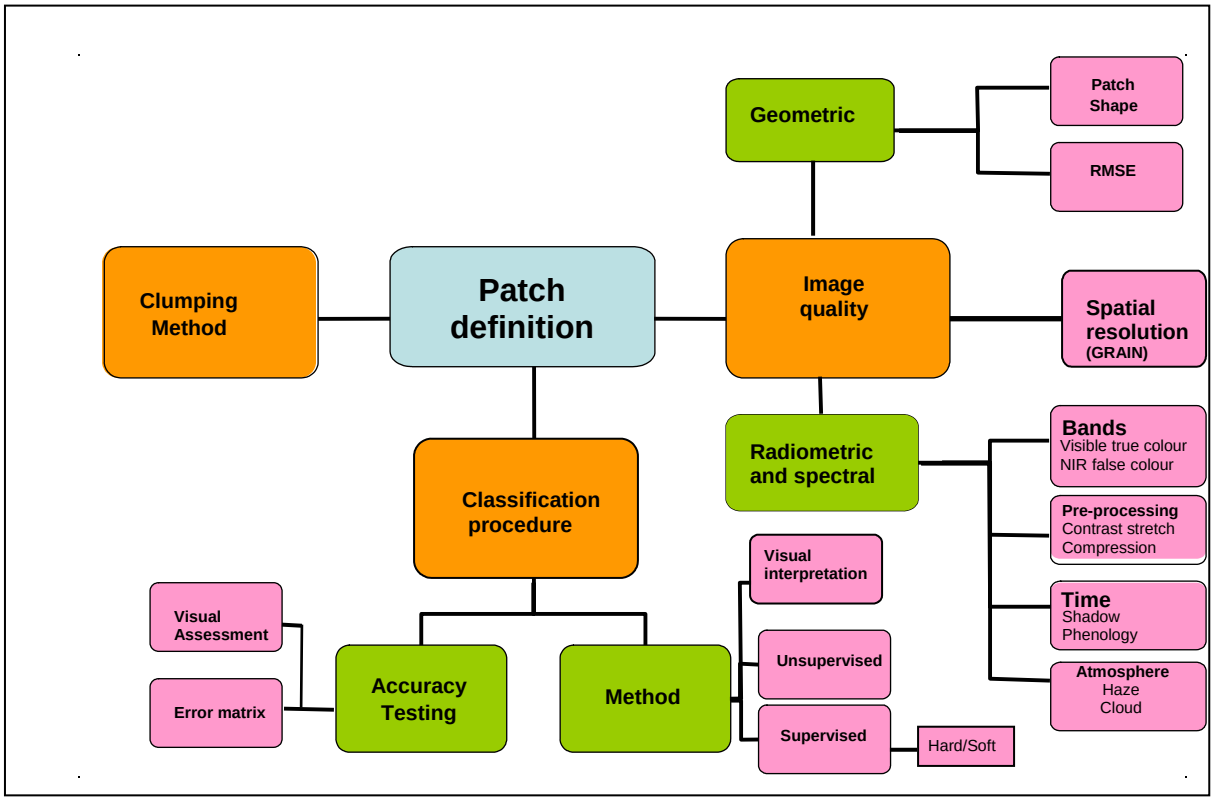

Figure 2.4: Factors affecting patch definition

3. IMAGE CLASSIFICATION

3.1 Methods

3.1.1 Rationale

A three class image was required from the aerial photographs, which could then be sieved and clumped to produce a patch map (section 4.1.1). The classes of interest here were exposed peat, mineral soil and vegetation.

A variety of classification methods are available from visual interpretation such as the work conducted by Bower (1960, 1961), to automated methods such as unsupervised and supervised multispectral classification. Multispectral classification allocates pixels in an image to thematic classes based on their reflectance in several parts if the electromagnetic spectrum (Casals-Carrasco *et al.*, 2000; Campbell, 2002; Dean and Smith 2003; Cihlar *et al.,* 1998*)*. The major advantage is that it has a repeatable framework that allows land managers to repeat the classifications over a number of timescales to monitor the progress of land management techniques (e.g. gully blocking or reseeding measures) or to assess the changes occurring in the landscape (e.g. as a result of fire).

3.1.2 Unsupervised classification method

Unsupervised classification schemes are fully automated procedures that classify data purely on their spectral properties with no prior knowledge of classes. It is quick but requires post-classification interpretation of the classes produced, which may not relate well to ground conditions. One of the main benefits of using an unsupervised classifier is that it enables spectral classes to be identified that may not be apparent to the analyst, in this case, the importance of shadow at Torside.

Unsupervised classification was carried out on all three datasets for both the TS and UNG catchments using the ISOCLUST program in Idrisi Kilimanjaro (Eastman 2003). Initially the optimum number of five classes was detected by the ISOCLUST program. Interpretation of the results against field knowledge resulted in grouping into three classes (peat, mineral soil and vegetation) based on interpretation of the aerial photographs. The combination of the classes which were merged varied with the imagery.

The time taken to run the program depends on the size and resolution of the imagery used and the specification of the computer being used. This is an important factor to take into consideration, as some computers may have difficulty processing large, high resolution imagery and the classification process may have to be split into a series of smaller images to be processed. For example, on a PC with 1GB RAM and a 3.06 GHz Pentium 4 Processor it took around 2 hours to complete one run. It is recommended that small extracts are used. In both cases, the catchment outlet point was defined by a gauging station. However, it would be preferable to use smaller, sub-catchments or isobasins (Lindsay *et al.,* 2005, sections 4.2 and 6.1).

3.1.3 Supervised classification method

Supervised classification requires user intervention and knowledge from the field sites in the form of training data prior to running the classification (Lillesand *et al*., 2004). It is more time-consuming but usually produces more meaningful results.

Kilimanjaro image processing software was used to run the maximum likelihood classification for the GM, UKP and NIR aerial photos and classify the images into Peat, Mineral Soil and Vegetation classes. The following sequences of operations were followed: (i) collection and definition of training/testing data from TS and UNG; (ii) extraction of signatures: (iii) classification of images.

(i) *Collection of training/testing data*

Torside was used instead of UNG to collect training data as it was the larger of the two catchments enabling a greater number of training areas to be selected. A total of 30 stratified randomly selected sites were identified (10 for each land cover type), spread across the whole catchment, to ensure that a high level of variability in each land cover type was accounted for. It is recommended that a total of 10 times as many pixels for each band in the image being classified should be collected for each class. Therefore, a minimum of 30 training pixels should be allocated per class as there are 3 bands available. At each point a minimum of five training/test areas, were recorded in the field. This was completed using a dGPS and by marking the areas on printouts of the aerial photographs. It is important to note that the size of the area selected needed to be clearly visible on the aerial photograph and therefore the majority of the areas selected were greater than 30 pixels. In practice the more sites and the larger the areas selected, the better the results tend to be. Out of all the areas collected, 70% were used for training and 30% for testing. The same method was repeated for the UNG catchment to provide a test data set for the UNG catchment. The training and test areas were digitised as polygons in IDRISI Kilimanjaro.

(ii) Extraction of signatures

The digitized training areas were used to extract signatures with the MAKESIG function of Idrisi Kilimanjaro (Eastman. 2003). Each signature contains statistical parameters for the pixels inside the training areas. It is obvious from the histograms for mineral soil (Figure 3.1) that the GM and UKP-TC images have been contrast stretched. The distribution is very negatively skewed, so that parametric techniques such as maximum likelihood classification are unlikely to work well for these two data sets.

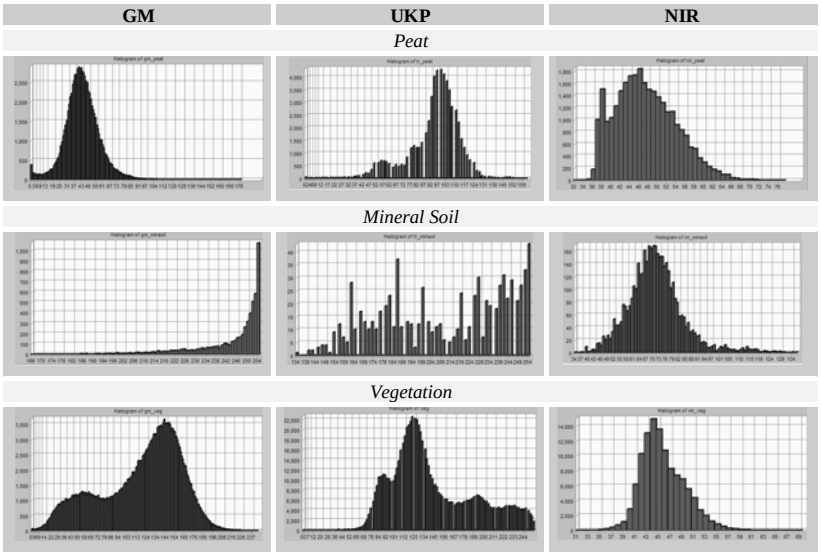

Figure 3.1: Frequency histograms of brightness values of training data for the three land cover classes for each of the image data sets.

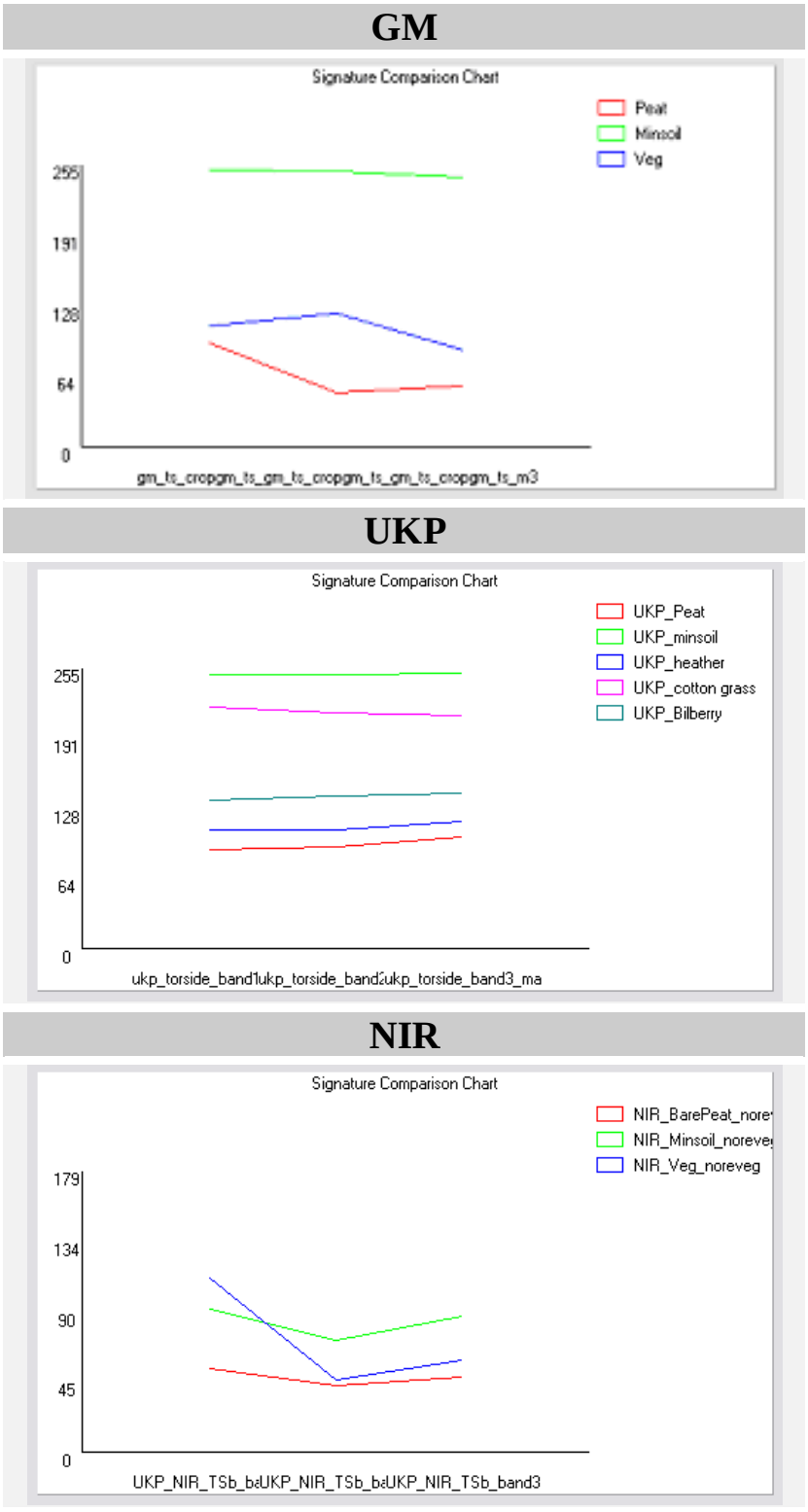

Figure 3.2: Signature comparison charts for the three data sets. GM and UKP-TC band order; blue, green, red. UKP-CIR band order NIR, red, green (i.e. reversed and beginning at longer wavelengths)

The signature comparison charts (Figure. 3.2) show that GM has the most distinct spectral responses, especially for peat, so is likely to produce a good classification. The UKP-TC signatures are the least separable, differing in brightness (albedo) and very little in shape (spectral signature). This would suggest that misclassification will be high for UKP-TC, especially where topography causes more differences in albedo which mask those between the land cover. For instance, mineral soil will be confused with cotton grass, and peat with heather.

In the UKP-CIR, vegetation has the most distinct signature, as expected. Peat is similar to mineral soil, differing mainly albedo so that sunlit peat slopes reflect similarly to shaded mineral soil. This suggests that the UKP imagery may have problems differentiating between the peat as and mineral soil.

Overall, the three classes are most separable for GM and least for UKP-TC. On spectral properties of the training data alone, GM is likely to produce the best patch maps. However, accuracy must be tested visually and quantitatively, and geometry must also be considered for pattern work.

(iii) Classification stage

The training data set is strong so the maximum likelihood method was used, as recommended by Richards (1995). The method assumes that the training data has a Gaussian normal distribution in all classes and all bands (Brown *et al.*1998), which was not the case for mineral soil in the GM and UKP-TC due to stretching (Figure 3.1), so poorer results were expected for these datasets. Idrisi Kilimanjaro's MAXLIKE was used to perform the classification (Eastman, 2003).

3.1.4 Masking

The catchment boundary was extracted from the LiDAR data and used to make a binary mask of zeros outside the catchment and ones inside it. The outlet point for the catchment was defined by the location of the gauging station[2]. The mask was multiplied by each unsupervised and supervised image to leave only the catchment classified, surrounded by black fill pixels.

3.1.5 Accuracy assessment

Accuracy of the classified images was first visually assessed by comparing against the aerial photographs and field knowledge.

A statistical accuracy assessment was also conducted for each image and type of classification using a ground truth image for each dataset constructed from independent test areas at which the actual land cover was known from fieldwork. Error matrices were produced showing the degree of correspondence between the class observed from fieldwork and the mapped class (from multispectral classification). The matrix summarises the errors of omission (the number of pixels in a class that have been omitted from a class) and errors of commission (the number of pixels added to a class in error). Overall accuracy is the sum of the principal diagonal in the error matrices and is the total of correctly classified pixels as a proportion of the number tested. The kappa coefficient describes the significance of the error matrices allowing for sample size. A value of 0.70 is regarded as good and indicates that the classification is 70% better than one occurring purely by chance (Mather 2004).

[2] The outlet point used to define the catchment in section 4 is actually 100m downstream of the gauging station hence the difference in catchment shape compared to those in this section.

3.2 Unsupervised Classification results

Unsupervised classification produced varying success for different catchment and data sources. The TS catchment will be discussed first followed by the UNG catchment.

3.2.1 Torside

Get Mapping

Unsupervised classification using GM (Figure 3.3(a)) produced a much poorer result at TS than at UNG (Figure 3.4(a)). Vegetation was under-estimated and misclassified as mineral soil (Figure 3.3(a), right-hand box), due to cotton grass having similar spectral properties to the mineral soil at this time of year. As with all most moorland vegetation types, the spectral reflectance of cotton grass changes seasonally, depending on whether it is producing new leaves, producing seeds or its leaves are senescent. This could explain why there are similarities in the signatures between the cotton grass and mineral soil. Some heather (Figure 3.3(a), left-hand box) has been misclassified as exposed peat class, due to shadow or recent burning that gives the heather a darker spectral appearance, thus over-estimating the peat class. As a result of these similarities in spectral properties, the unsupervised classifier has difficulty separating the classes so inaccuracies occur. The overall outcome is that unsupervised classification produces a poor land cover map. The error statistics confirmed that this was the case (section 3.4).

UKP True colour

The UKP-TC images (Figure.3.3(b)) produced a much better unsupervised classification at TS than the GM discussed above (Figure 3.3(a)). The mineral soil was more realistically mapped, with few problem areas, as in the northern part of the catchment where, once again, cotton grass has been misclassified as mineral soil. There is also a large area of dwarf shrub heath vegetation and some rock outcrops at Torside Clough in the far left of the image that were misclassified as peat (white box in Figure 3.3(b)). This area is in shadow, which reduces reflectance in all bands and makes the spectral properties of the vegetation similar to those of exposed peat. Supervised classification methods that use training areas to identify the specific classes may help to reduce this problem of misclassification in the shadowed areas although may not eradicate the problem altogether. In fact, this was a major problem that recurred for TS in all the image datasets and with all classification methods and proved impossible to rectify in the time available.

Overall, the UKP-TC imagery produced a reasonable unsupervised classification. Mineral soil distribution was much more accurate, but the over-estimation of exposed peat would create problems when using the patches to analyse the spatial patterns of erosion risk (section 5.5).

UKP colour infrared

The UKP-CIR imagery (Figure 3.3(c) produced the best of the three unsupervised classifications due to the better discriminatory power of the near infrared band. The peat class was more representative of the exposed peat but peat was still over-estimated, mainly in deeply shadowed area of vegetation (Figure.3.3(c), top left box) This problem however, is greatly reduced compared to the UKP-TC imagery. In addition, mineral soil was slightly over estimated as illustrated by the right-hand box, possibly due to confusion with burned peat.

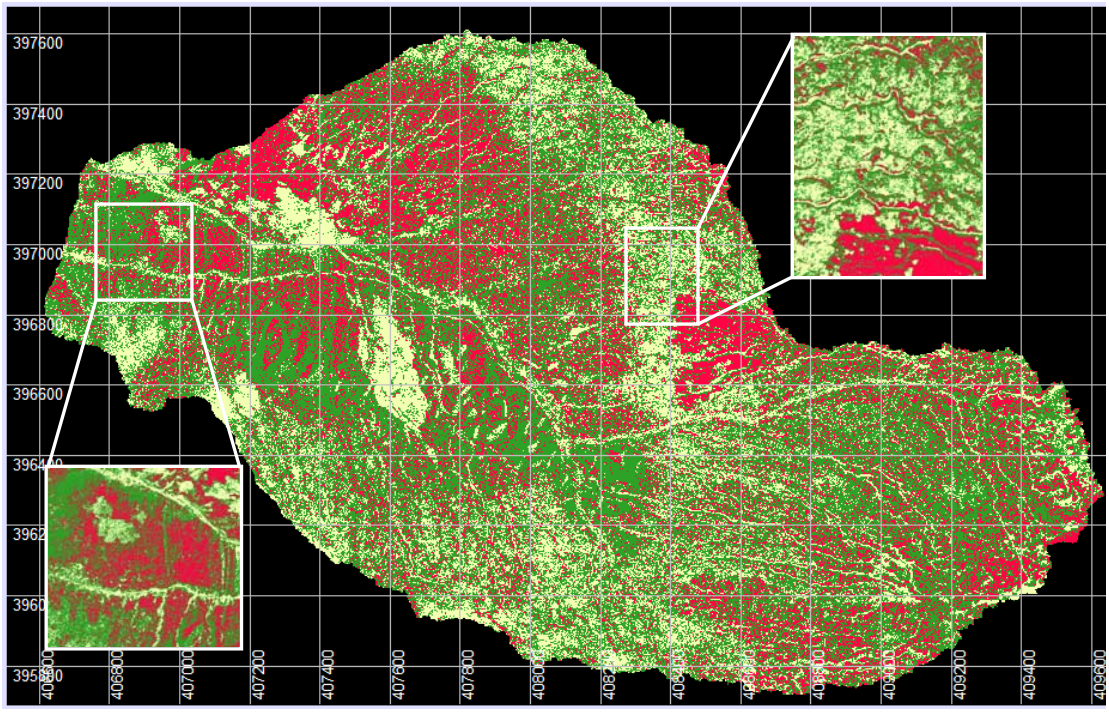

Figure 3.3 (a): Unsupervised classification for Torside using Get Mapping aerial photographs. Red = Exposed Peat, Yellow = Mineral soil and Green = Vegetation.

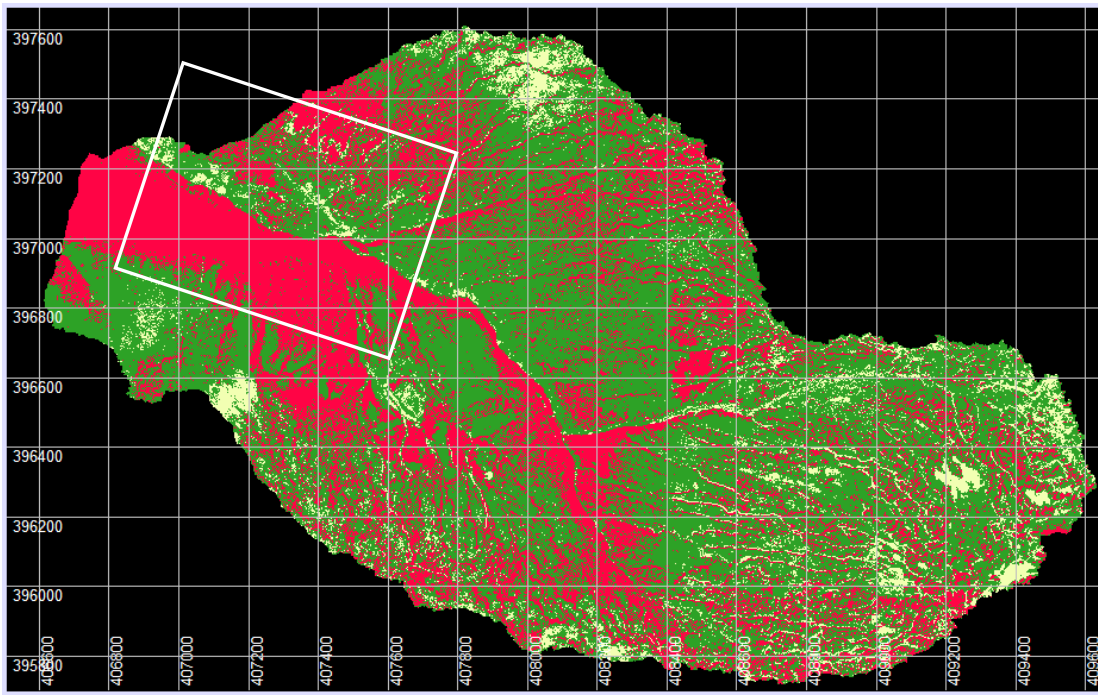

Figure 3.3(b): Unsupervised classification for Torside using UKP true colour aerial photographs (1997-2001). Red = Exposed Peat, Yellow = Mineral soil and Green = Vegetation.

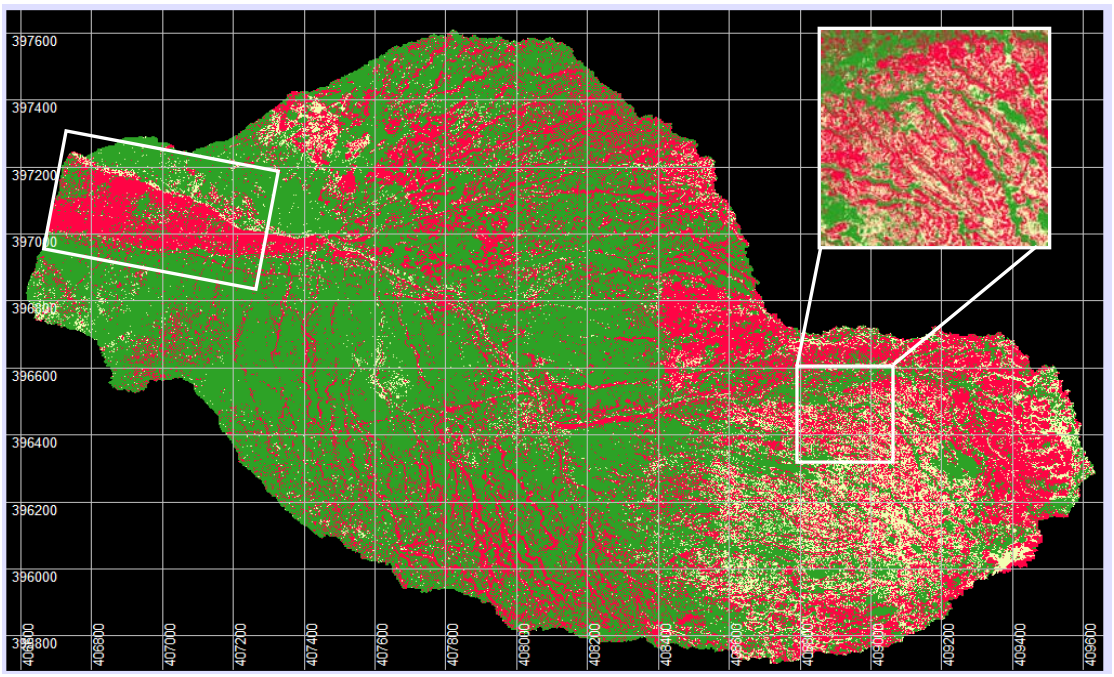

Figure 3.3(c): Unsupervised classification for TS using UKP colour infrared aerial photographs. Red = Exposed Peat, Yellow = Mineral soil and Green = Vegetation.

3.2.2 Upper North Grain

Get Mapping

The GM imagery results were realistic for the eastern part of the catchment. The right-hand box of Figure 3.4(a) shows a mineral-floored gully with exposed peat walls and extensive areas of mineral soil to the east, representing an advanced stage of erosion. The classification also accurately reflected peat floored gullies, which represent an early stage of incision, and gullies with (re-)vegetated floors, indicating trapping of sediment. However, in the north western part of the image a large area of cotton grass was misclassified as mineral soil (Figure.3.4 (a), left-hand box).

UKP true colour

The UKP-TC images (Figure 3.4 (b)) produced poor results and could not be used for further analysis. Large areas of vegetation were misclassified as exposed peat and cotton grass was classified as mineral soil. Exposed peat (Figure 3.4(b), box) in gully walls was over-estimated due to shadow.

UKP colour infrared

The UKP-CIR produced a much better classification than the other two data sets (Figure 3.4(c)). Peat floored gullies are clearly identified and the amount of peat identified is more realistic, although slightly under-estimated in favour of vegetation This may be due to the fact that certain areas of the peat are naturally revegetating so that the spectral properties of the peat are more like vegetation, an issue addressed in section 3.5. Cotton grass misclassification has been greatly reduced compared to GM and UKP-TC and the vegetation class was more representative.

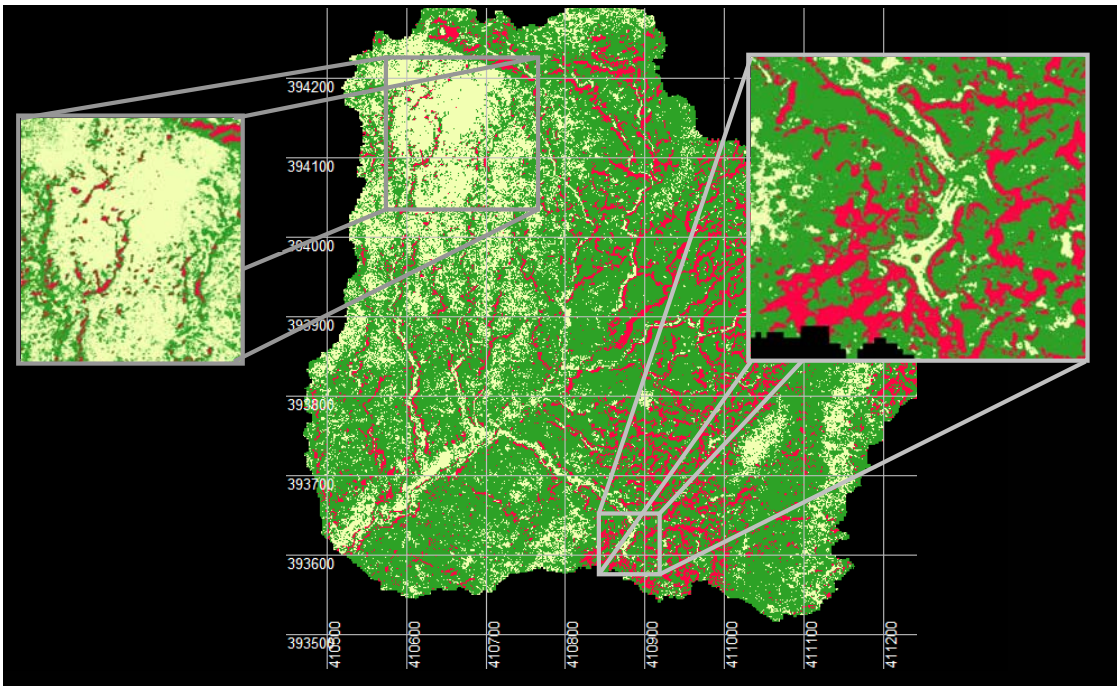

Figure 3.4(a): Unsupervised classification of Upper North Grain using Get Mapping true colour aerial photographs. Red = Exposed Peat, Yellow = Mineral soil and Green = Vegetation.

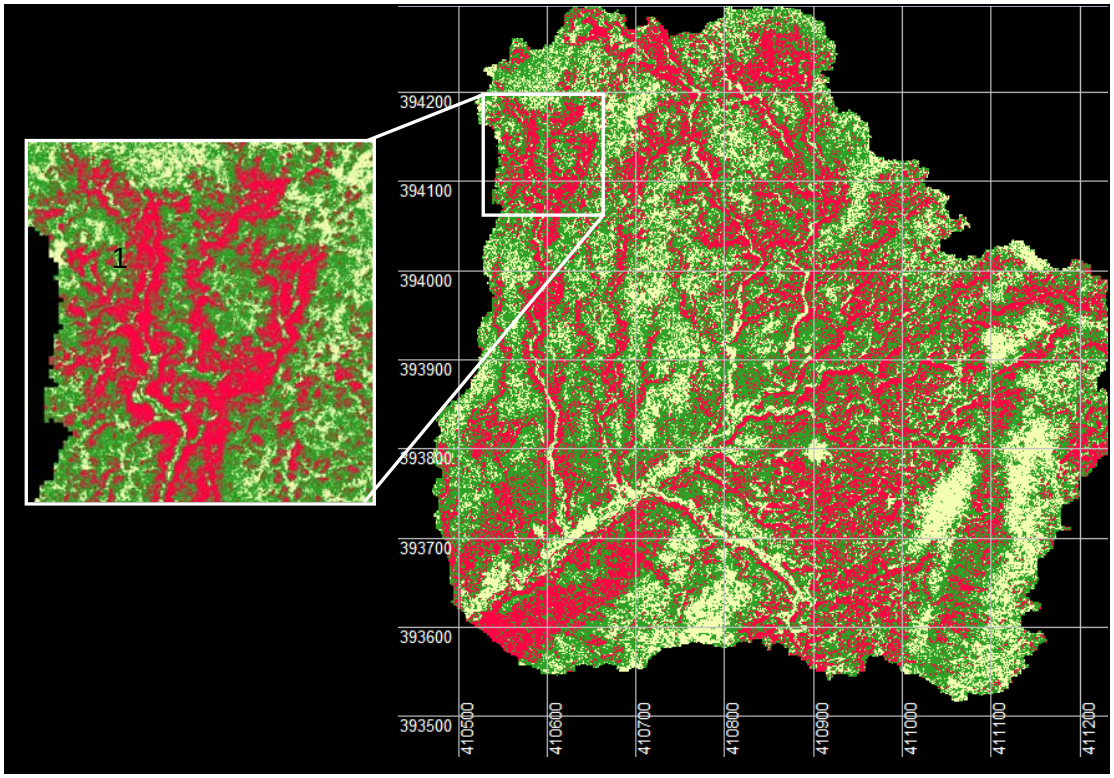

Figure 3.4(b): Unsupervised classification of Upper North Grain using UKP true colour aerial photographs (1997-2001). Red = Exposed Peat, Yellow = Mineral soil and Green = Vegetation.

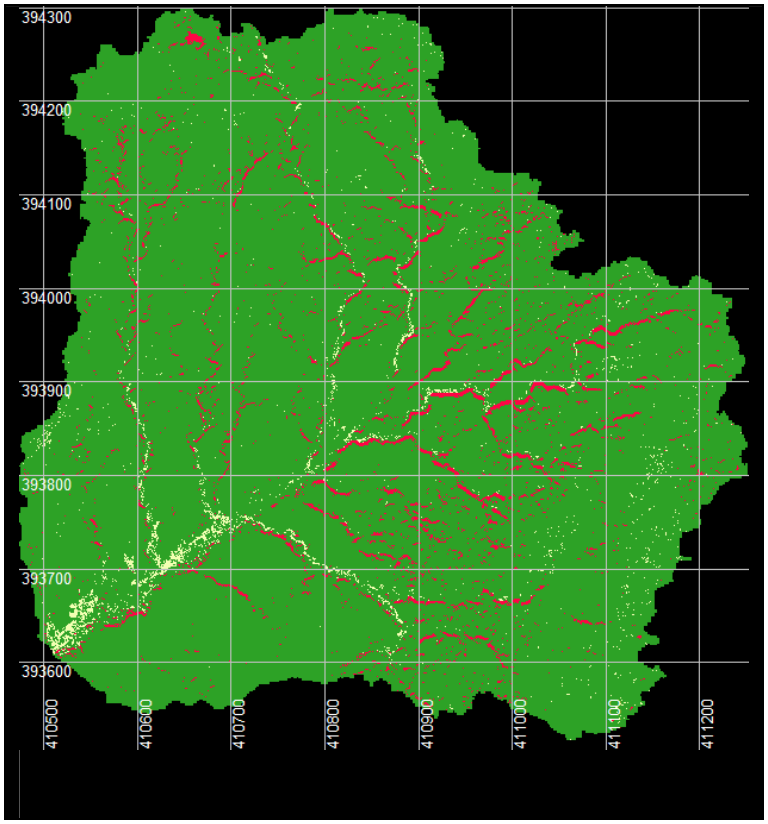

Figure 3.4(c): Unsupervised classification of Upper North Grain using UKP colour infrared aerial photographs. Red = Exposed Peat, Yellow = Mineral soil and Green = Vegetation.

3.3 Supervised Classification Results

The supervised classification results visually were much better than the unsupervised. All classes in all three images were more realistic and problems with shadow were reduced although not entirely eradicated.

3.3.1 Torside Clough

Get Mapping

Supervised classification of the GM imagery was initially carried out using only three classes. Results were good, with bare peat and mineral soil representing the landscape well. However, in the first attempt (not illustrated here) some areas of peat were misclassified as vegetation, therefore, an additional peat class (burnt peat) was identified to more fully represent the variability in peat reflectance. The two peat classes were merged to form a single peat class post-classification. Improving the training data set by refining the other classes and adding a new peat class has enabled a more representative training data set to be produced allowing for a more accurate classification (figure 3.5(a)). Misclassification of pixels was greatly reduced compared to unsupervised results.

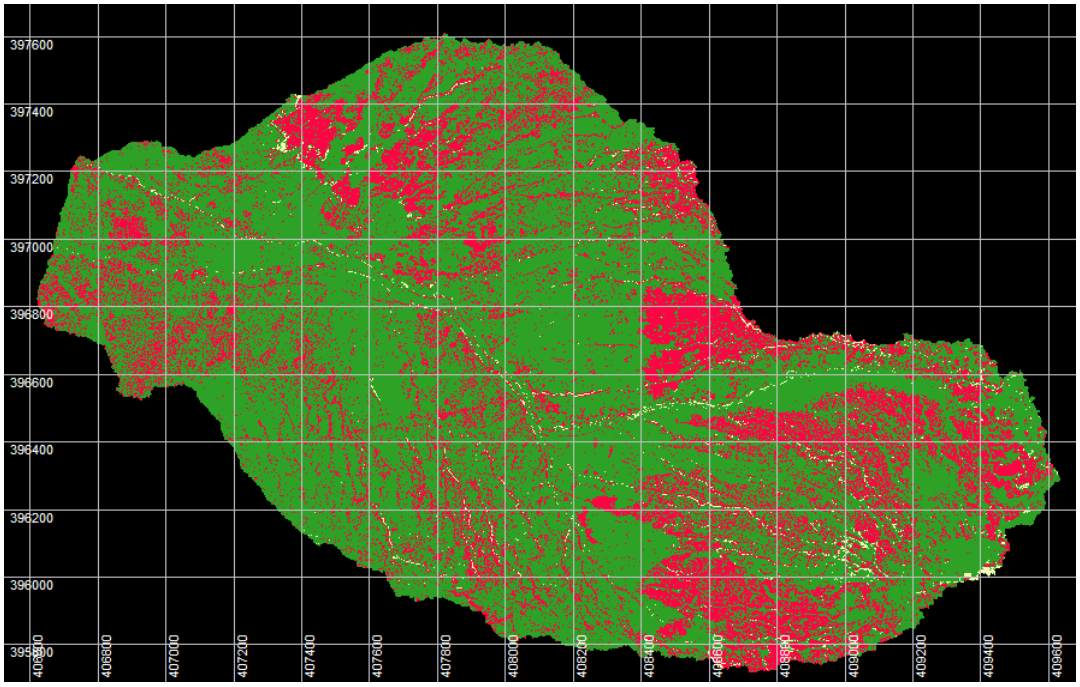

Figure 3.5(a): Supervised maximum likelihood classification of TS using Get Mapping aerial photographs. Red = Peat, Yellow = Mineral soil and Green = Vegetation.

UKP true colour

The UKP-TC imagery proved to be more difficult and problematic to classify, as expected due to the artefacts and compression issues. First attempts using three classes were largely unsuccessful. Large areas of vegetation were misclassified as peat and mineral soil. Attempts to improve the classification included re-digitization of the training data and splitting the vegetation class into three separate classes (veg 1, veg 2,

and veg 3), creating a total of 5 classes. After classification, the vegetation classes were reclassed to a single vegetation class. This greatly improved the classification, although there was still a large area of vegetation in shadow misclassified as peat (white box in Figure 3.5(b)). Peat in this imagery varied little in the spectral range so only one peat class was used, unlike in the GM imagery. The outcome was a reasonable classification; however, the over-estimation of peat in the large shadowed area was still cause for concern.

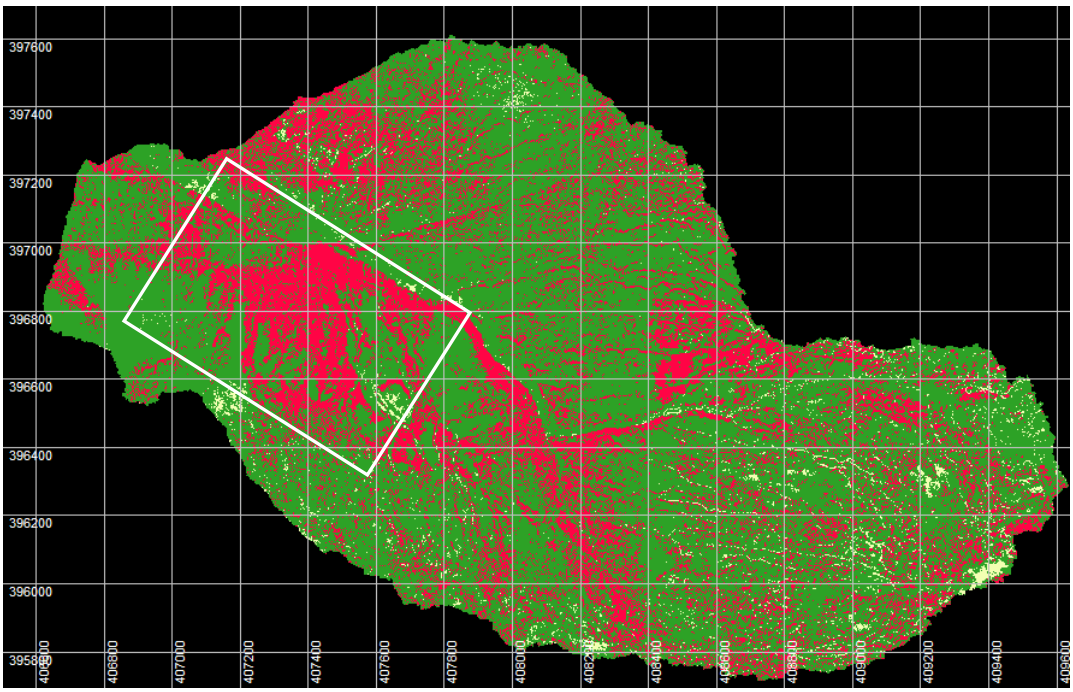

Figure 3.5(b): Supervised classification maps of TS using UKP true colour aerial photographs (1997-2001). Red = Exposed Peat, Yellow = Mineral soil and Green = Vegetation.

UKP colour infrared

It is important to note that at the time the UKP-CIR imagery was flown in 2005, some reseeding work had been carried out in the TS catchment to revegetate exposed peat areas. It is therefore important that these areas are clearly identified so a fourth class (revegetated peat) was included in the classification. As this project is interested in peat prior to reseeding, this class was reclassed as peat after classification. In addition, other management measures carried out in the TS catchment involved laying down geojute matting on the gully walls of exposed peat. to stabilize the peat surface, inhibit the removal of peat into the channel and help prevent the new seeds being blown away.

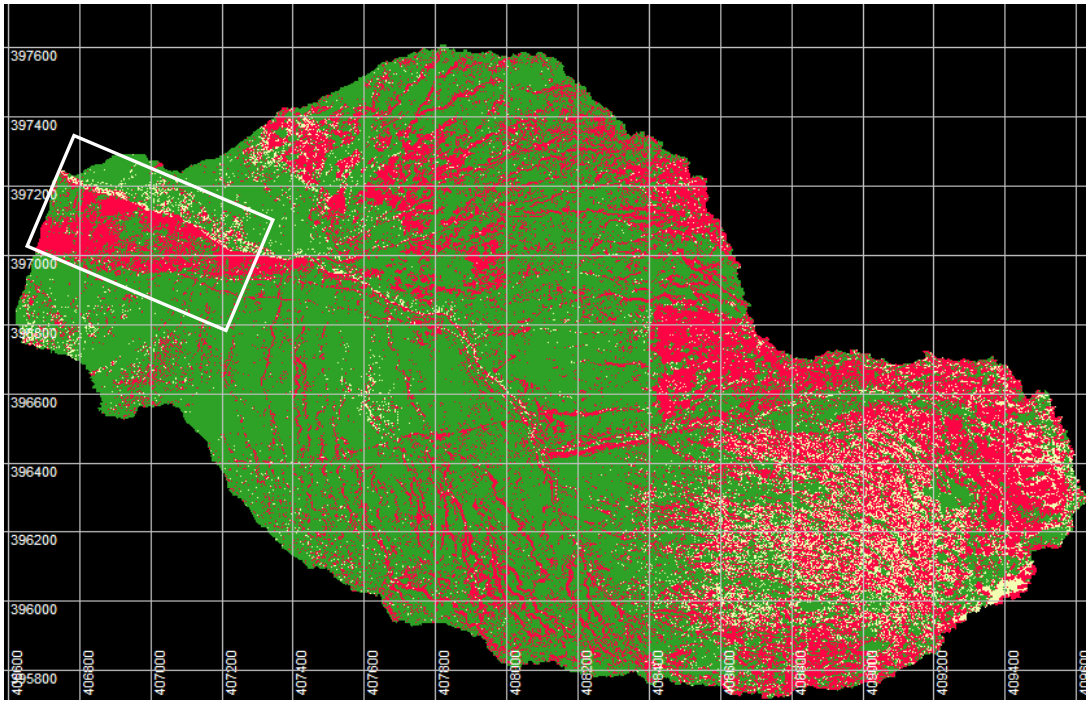

Figure 3.5(c): Supervised classification of TS using UKP-NIR. Red = Peat, Yellow = Mineral soil and Green = Vegetation.

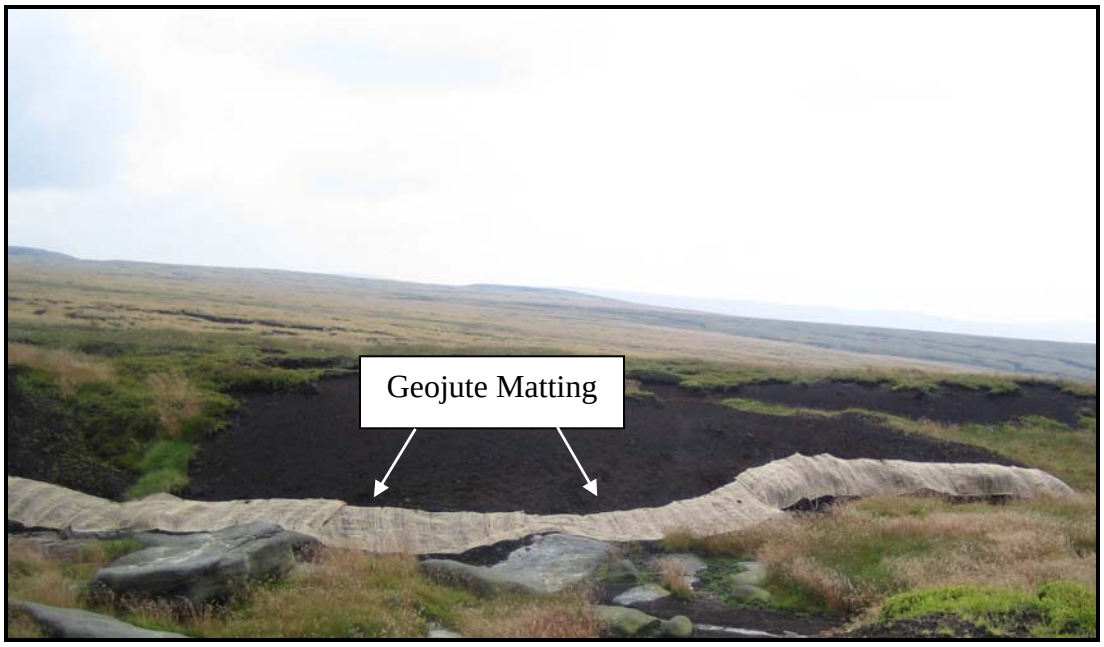

Figure 3.6: Geojute matting on peat walls in the Torside catchment.

Geojute (Figure. 3.6) was misclassified as mineral soil. As the map was intended to show the baseline situation prior to restoration, these areas had to be identified and reclassed as peat. It was assumed that the geojute areas were uniform and wider,

whereas mineral soil areas was characterised by much thinner, more discontinuous bands. Areas of the image where geojute could be visually recognised were masked off and pixels within them forming bands of above a critical threshold width were reclassified as geojute. These were then added back to the rest of the classified image (Figure 3.7) and finally reclassed as peat. The Idrisi procedure is shown in the flow chart Figure 3.8.

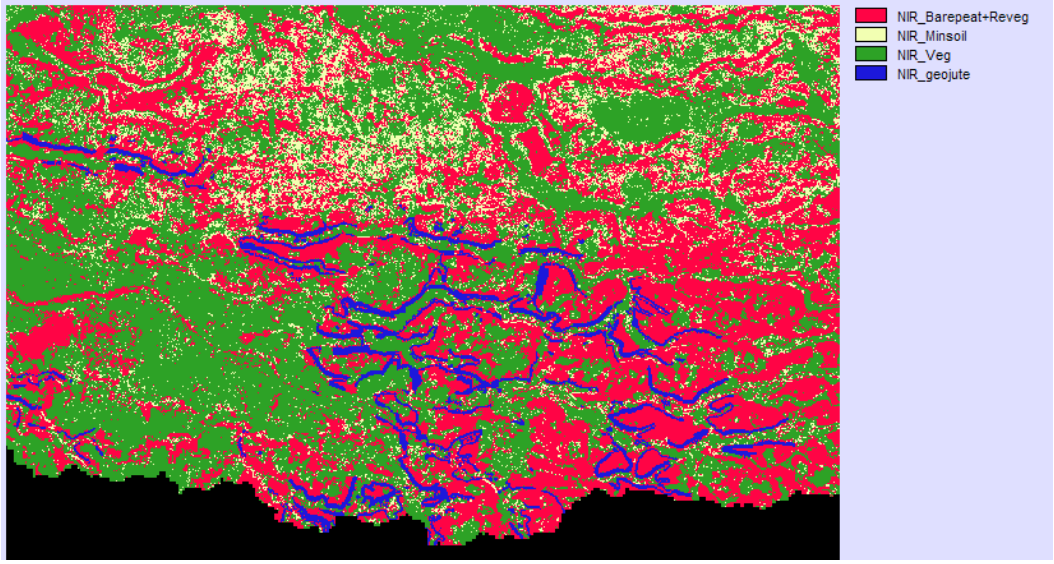

Figure 3.7: A geojute area in the TS catchment, to the northwest of Bleaklow Head. Mineral soil forming bands below a critical width were identified as geojute (step 10 in Figure 3.8) before being reclassed as peat to represent pre-restoration condition.

Initial interpretation after the reseeded areas and geojute had been dealt with, suggested that the classification of the UKP-CIR imagery represents the landscape reasonably well. The same shadowed area located in the white box in figure 3.5(c) is a problem as is misclassification of burnt peat as mineral soil in Joseph's patch (figure 5.4).

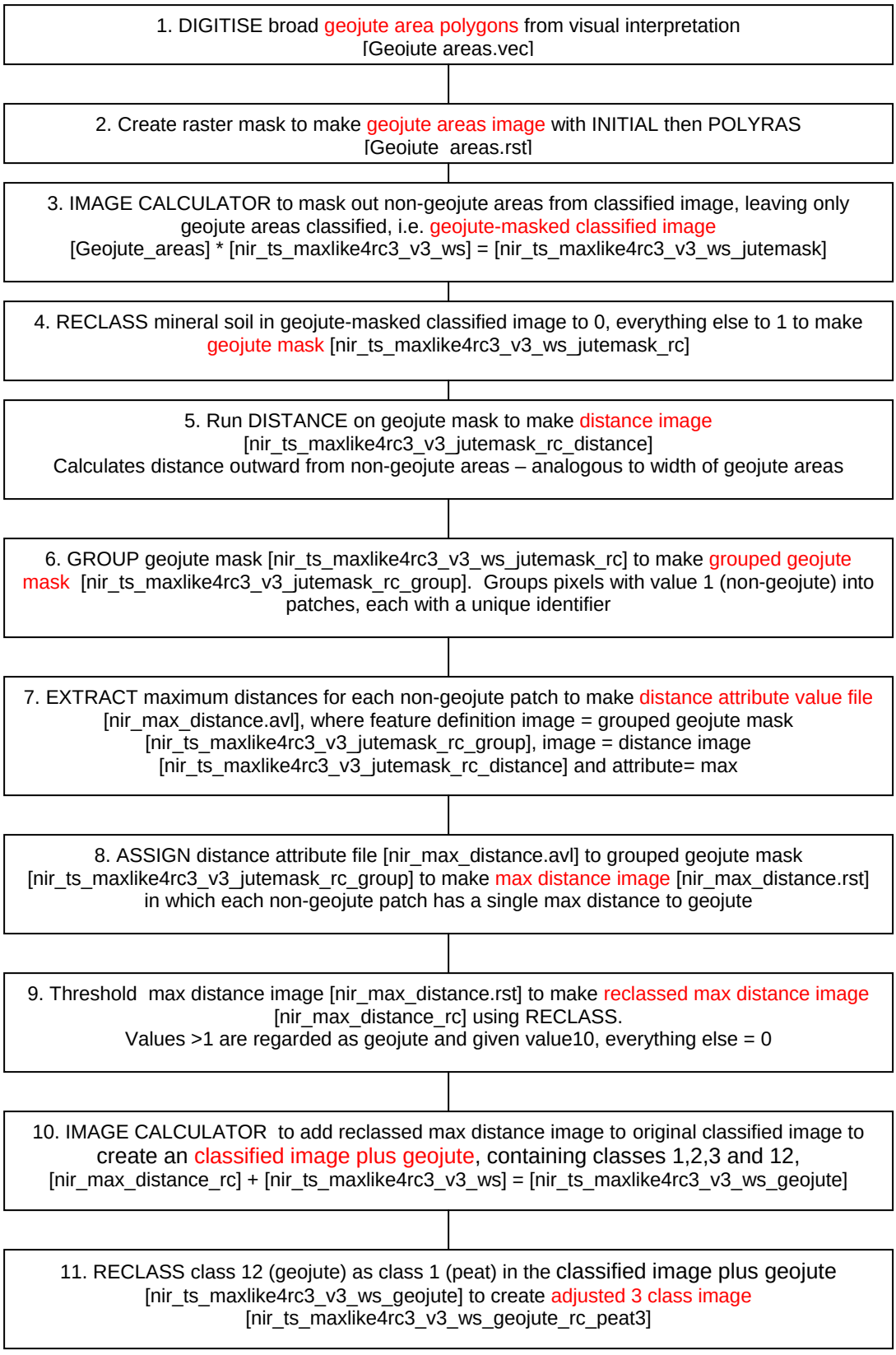

Figure 3.8: Flowchart showing steps to identify mineral soil which is actually geojute-covered peat on UKP-CIR classified image and reclass them as peat.

3.3.2 Upper North Grain

Once the TS classifications had been carried out, the signatures produced for each of the datasets in the TS catchment were used to classify UNG. As the area does not contain burnt peat or reseeded areas, only the signatures for the first three initial classes (exposed peat, mineral soil and vegetation) were used.

Get Mapping

The GM mapping classification of UNG (Figure. 3.9(a)) worked well. Misclassification of cotton grass as mineral soil was greatly reduced compared to unsupervised results. Peat-walled gullies that are characteristic of this catchment have been clearly identified, as have and mineral-floored gullies. However, the peat may have been over-estimated in places due to shadow on gully walls, but under-estimated for sunlit peat walls of gullies. As the shadowed gully walls are usually also peat, they have been correctly classified, but little could be done to redress the sunlit problem other than have two peat classes, sunlit and shaded.

Overall, it could be said that the signatures taken from the GM classification of the TS catchment represent the variability in the land cover types in UNG. However, signatures taken from the UKP-TC and UKP-NIR classification of TS did not work as well in classifying the equivalent UNG dataset.

UKP true colour

UKP-TC imagery produced a reasonable result although vegetation (cotton grass) was again over-estimated and misclassified as mineral soil (Figure. 3.9(b)). This could be due to the quality of the imagery, but also a result of the time of day and season (late summer) the dataset was flown. Peat has been identified well and many of the peat-walled gullies can be clearly located.

This suggests that the TS signatures produced for UKP-TC imagery have worked reasonably well in identifying the land cover patches in UNG, but do not cover the full variability in the vegetation. Further experimentation with more training areas may improve this, however, the problem is a partly a result of compression artefacts and stretching, so effort was directed at improving results from the UKP-CIR dataset.

UKP colour infrared

The NIR imagery produced some unexpected results (Figure. 3.9(c)). Signatures from TS did not transfer well, suggesting that they did not represent the full variability in the land cover types. This is to be expected as the NIR band would emphasise differences in vegetation and peat between catchments which were not seen at visible wavelengths.

Peat classified reasonably well but its spectral properties were more closely matched to the signatures produced for revegetating peat at TS. Therefore, the revegetating peat signature was tried in place of the original exposed peat signature. Mineral soil was largely over estimated; misclassified pixels should have been vegetation.

A new set of training areas within the UNG catchment were drawn and the classification was re-run. Mineral soil was still over-estimated (Figure. 3.9(c)), so prior probabilities were adjusted to increase the chances of misclassified pixels being assigned to the correct class. Mineral soil was given a low probability and vegetation a high probability.

This simple method worked well. The remaining misclassified pixels are a scattering of single pixels that can be sieved out with a filter reclassing them to the group having the longest shared boundary (section 4.1.1).

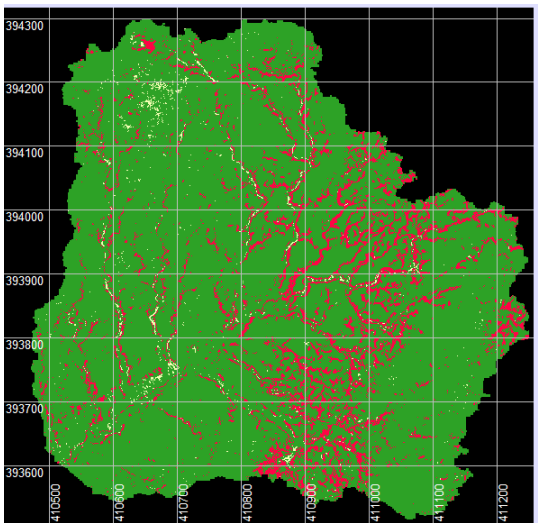

Figure 3.9(a): Supervised classification of UNG using UKP true colour aerial photographs (1997-2001). Red = Peat, Yellow = Mineral soil and Green = Vegetation.

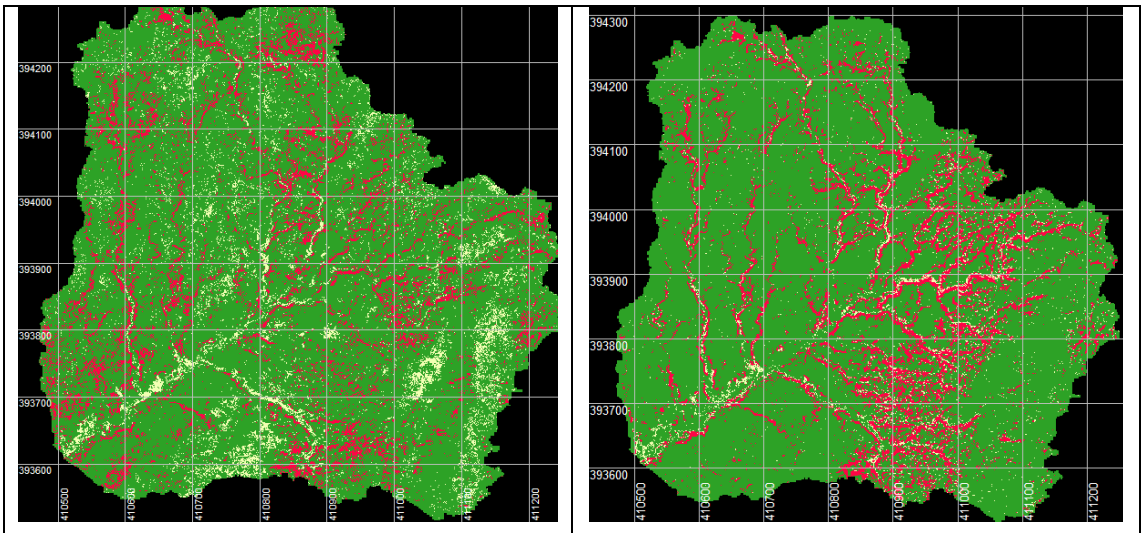

(b) *(c)*

Figure 3.9(b): Supervised classification of UNG using GM true colour aerial photographs (1997-2001). Red = Peat, Yellow = Mineral soil and Green = Vegetation.

Figure 3.9(c): Supervised classification of UNG UKP colour infrared aerial photographs. Red = Peat, Yellow = Mineral soil and Green = Vegetation.

3.4 Results of statistical Accuracy Assessment

Table 3.1 summaries the overall accuracy of the classified maps and provides the Kappa index for each image. Supervised classification produced more accurate results than the unsupervised methods, as expected. The UKP-CIR produced the highest accuracy for UNG. GM had the highest accuracy for TS, closely followed again by UKP-CIR. The UKP-TC imagery produced the poorest results for both the unsupervised and supervised methods.

Tables 3.2 and 3.3 provide examples of the error matrices, in this case, for supervised classifications of the UKP-CIR imagery. The major sources of error for both catchments are for class 2 (mineral soil). The high errors of commission and omission are largely due to the small number of test pixels available. The amount of mineral soil found within both catchments is, proportionately, much lower than the other two classes, making it difficult to locate a high number of test areas. However, the overall accuracy for both maps is considered to be of a good standard.

Statistical accuracy assessment suggests that either the GM or UKP-CIR imagery should be used to produce patch maps for encoding erosion pattern. However, when geometric accuracy is also taken into account, the UKP-CIR is the best currently available source. Although the classification results for GM are good, geometric properties are too poor to be used for identifying connectivity of patches to the channel network.

Table 3.1: Thematic error statistics for each classification

Image Source	Catchment	Statistic	Unsupervised	Supervised
GM	TS	Overall error	0.5343	***0.0537***
		Kappa	0.1928	***0.8429***
	UNG	Overall error	0.4277	0.0154
		Kappa	0.0506	0.7638
UKP-TC	TS	Overall error	0.3893	0.4722
		Kappa	0.3515	0.1732
	UNG	Overall error	0.8116	0.6567
		Kappa	0.0229	0.0327
UKP-NIR	TS	Overall error	0.0919	0.0705
		Kappa	0.7261	0.7837
	UNG	Overall error	0.4312	***0.0083***
		Kappa	0.1199	***0.9083***

Table 3.2: Error Matrix for TS using UKP-CIR

Columns = observed in field, Rows = mapped on classified image

	1 Peat	2 Minsoil	3 Veg	Total	Error C
0 Unclassified	456	1041	0	1497	1.0000
1 Peat	5477	160	859	6496	0.1569
2 Minsoil	55	400	445	900	0.5556
3 Veg	5	0	33949	33954	0.0001
Total	5993	1601	35253	42847	
Error O	0.0861	0.7502	0.0370		**0.0705**

Overall Kappa = 0.7837

ErrorO = Errors of Omission (expressed as proportions)
ErrorC = Errors of Commission (expressed as proportions)

90% Confidence Interval = +/- 0.0020 (0.0685 - 0.0725)
95% Confidence Interval = +/- 0.0024 (0.0681 - 0.0729)
99% Confidence Interval = +/- 0.0032 (0.0673 - 0.0737)

Table 3.3: Error Matrix Analysis for UNG using UKP-CIR

Columns = observed in field, Rows = mapped on classified image

	1 Peat	2 Minsoil	3 Veg	Total	Error C
1 Peat	970	8	28	1006	0.0358
2 Minsoil	24	224	117	365	0.3863
3 Veg	24	33	26674	26731	0.0021
Total	1018	265	26819	28102	
Error O	0.0472	0.1547	0.0054		**0.0083**

Overall Kappa = 0.9083

ErrorO = Errors of Omission (expressed as proportions)
ErrorC = Errors of Commission (expressed as proportions)

90% Confidence Interval = +/- 0.0009 (0.0074 - 0.0092)
95% Confidence Interval = +/- 0.0011 (0.0073 - 0.0094)
99% Confidence Interval = +/- 0.0014 (0.0069 - 0.0097)

3.5 Discussion and Summary

Having assessed both radiometric and geometric image quality and thematic accuracy for each of the data sets, the UKP-CIR imagery was selected for mapping and encoding the spatial pattern of peat erosion. The NIR band separates the vegetation from the peat better. It can therefore be recommended that any further imagery obtained should contain the NIR band. It is also important that all future imagery is fully orthorectified to enable geometric error to be kept to a minimal. This will enable the aerial photos and products extracted from the remotely sensed data to be used in conjunction with other datasets such as LiDAR.

By combining topographic information with image data, it maybe possible to improve classification results, especially where land cover types have similar spectral properties (e.g. heather and peat, cotton grass and mineral soil, geojute and mineral soil) but different topographic associations. They may be situated on very different elevations, slopes or aspects. Therefore, by combining slope, elevation or aspect layer in the classifier, ambiguities may be resolved (Jones *et al.,* 1988, Lillesand *et al.,* 2004).

To reduce the shadow and sunlit slope problem, either ratios or a simulated illumination layer derived from the DEM could be included, or full topographic normalisation could be carried out (Ekstrand, 1996).

Another possible option is to use airborne scanner imagery that use a greater number of narrower spectral bands which maybe able to separate the classes better. Scanners incorporating the near infrared and shortwave infrared parts of the electromagnetic spectrum, such as the NERC Airborne Thematic Mapper, should reduce thematic classification error. Use of hyperspectral sensors such as CASI with its many narrow bands (good spectral resolution) would also be expected to reduce error, especially for reseeded peat. The SPECIM AISA Eagle and Hawk flown on 13 July 2006 combines the two advantages of spectral range and resolution (NERC ARSF, 2006).

The classified images have a number of potential uses. First, they can be used to visually identify areas of significant erosion and potential problem areas. Second, they can be used to encode pattern quantitatively and, when combined with a good quality DEM, used to derive erosion metrics (section 4).

They can be used as the baseline from which to judge the success of management techniques. However, images produced by a simple three class hard classification will not be suitable for monitoring restoration works, whether the rate of revegetation after reseeding areas, the rate at which new vegetation grows through geojute, or the success of gully blocks in revegetating gullies. As natural and managed revegetation progresses, the spectral signature will be mixture of peat and vegetation, or peat and (mineral soil-like) geojute. Additional intermediate classes of revegetating peat will have to be used (as here).

A more appropriate alternative would be soft classification, including fuzzy classification and spectral unmixing (Foody, 1996 and 2000; Mehner *et al*., 2004). Unlike hard classification, pixels are not forced to belong to a single class. Instead, a three class soft classifier would produce three grey-scale images showing the probability of belonging to peat, mineral soil or vegetation. Spectral unmixing, would produce estimates of the relative proportions peat, mineral soil and vegetation in each pixel, that is, fractional cover, analogous to percent cover in a plot. These methods are more difficult to implement, since most require 'pure' pixel training data (e.g. pixels which are 100% peat). It is also more difficult to make a quantitative assessment of classification accuracy.

Linear unmixing methods were tried for a sub-catchment at Torside. Promising results were obtained, but the approach has limited value for encoding pattern, because the output had to be thresholded to produce a simple three class map. However, given more time, the mean probability of membership to the peat class (or measures of central tendency and dispersion for that membership) could be extracted for each patch as a way of expressing thematic classification error.

Other alternatives to multispectral classification which could usefully be explored include artificial neural networks (ANN) and support vector machines (Berberoglu *et al*., 2000; Huang *et al.,* 2002; Keramitsoglou *et al*., 2006; Pal and Mather, 2005).

4 ENCODING

4.1 Methods

The 3-class image was imported from IDRISI to TAS GIS, a freely available GIS package (http://www.sed.manchester.ac.uk/geography/research/tas/) specifically designed for environmental modelling and terrain analysis (Lindsay, 2005). TAS was used to extract all of the patch metrics and for pre-processing of the class image.

4.1.1 Pre-processing the Class Image:

The 3-class image contained numerous small patches that were a few grid cells in size. Although this occurs very commonly image classification procedures, these small patches are irrelevant from a management perspective. Furthermore, processing an image containing numerous patches adds considerably to the complexity of analyses and database size. In some cases, this can make analysis of any resulting database impossible. This problem is frequently handled by passing a modal filter over the image, i.e. a filter that replaces the grid cell at the centre of a roving kernel with the most frequently occurring class within the kernel. This approach suffers from several problems: i) it modifies all patch boundaries within the image, regardless of their size, ii) it cannot be guaranteed that all small patches are removed, and iii) new small patches can be created as a result of the filter. Thus, an alternative approach was developed for this work to eliminate small patches.

Figure 4.1 describes the sieve procedure used to remove small patches from the class image without affecting patch boundaries. A TAS GIS script was also developed to automate the procedure for future use (Table 4.1).

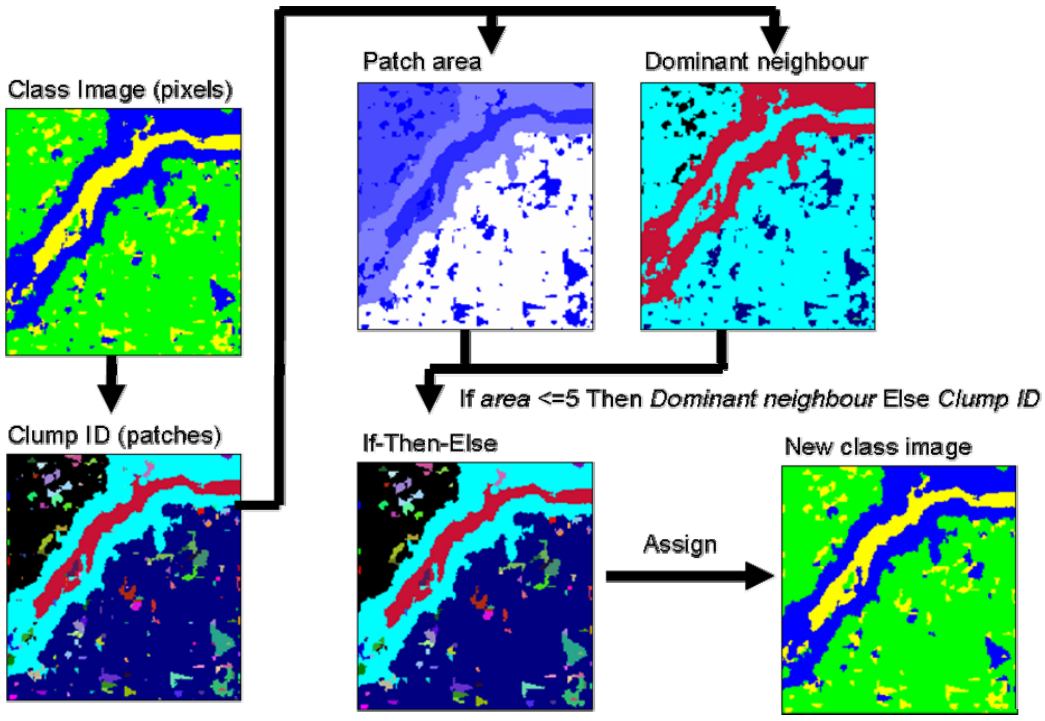

Figure 4.1: Procedure used to sieve small patches from the classified image.

Table 4.1: TAS GIS script for automation of the sieve procedure.

```
//TAS GIS script for performing a sieve to remove small patches from a class image.
//Inputs are the class image name and the threshold size.
//Outputs are the cleaned class image and a new patch ID image.

//Written by John Lindsay, July 24, 2006.

image = 'ENTER CLASS IMAGE NAME HERE'*1  //Renames the class image
old patch ID = CLUMP('image',true)
patch area = AREA('image',false)
NWLSB = NEIGHBOURPATCH('old patch ID',false)
thresholded image = IF('patch area'<=5,'NWLSB','old patch ID')
//Change the threshold value in last line as required
final class image = EXTRACTSTATS('image','thresholded image',dominant,false,(-9999))
//This last line is equivalent to an ASSIGN operation
final patch ID = CLUMP('new class image',true)
```

The sieve procedure required development of a new algorithm to calculate the neighbouring patch with the longest shared boundary, i.e. the 'dominant neighbour' (Figure 4.2). This algorithm is not available in GIS packages other than TAS.

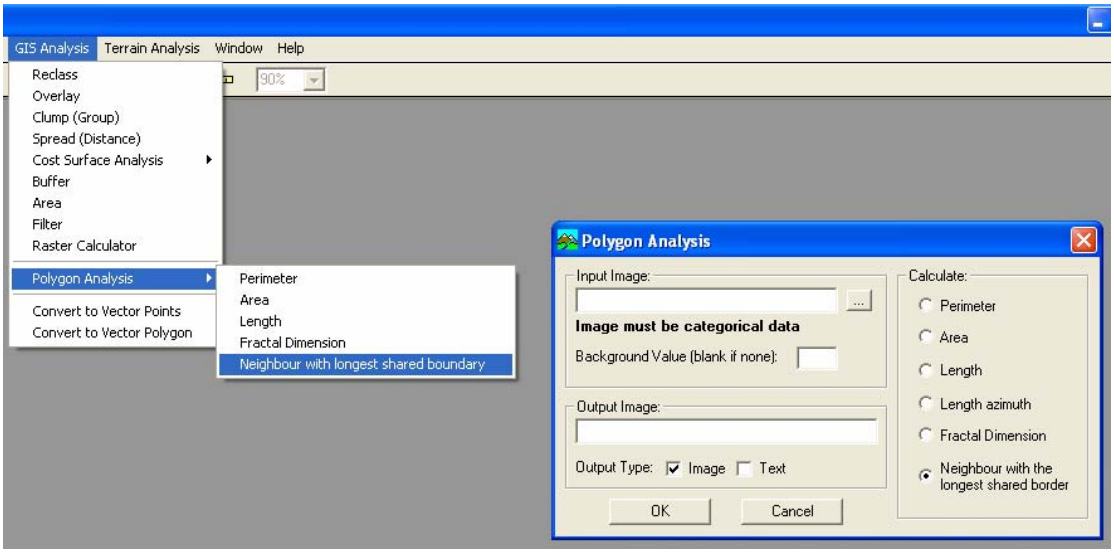

Figure 4.2: The new neighbour with the longest shared boundary algorithm in the TAS GIS software.

The result of the sieve procedure is a new class image in which all grid cells that are less than a user-specified threshold are assigned the class value of the patch in which they are embedded. A threshold of 5 grid cells, or 6.25 m^2, was used in this work. For the Torside catchment, this threshold value resulted in a reduction in the number of patches from 302,565 to 62,143. Sieving reduced the number of patches for UNG catchment from 28,404 to 5130. Notice that the number of patches in the original class map of Torside catchment (Fig 3.5(c)) would have been prohibitive for statistical analysis in most software packages.

A final Patch ID map was created from the new class image resulting from the procedure outlined in Figure 4.1 by using the clump (group) algorithm. It should be noted that 8-cell connectivity was used in all clumping procedures, i.e. diagonals were used to group patches together. These final patch IDs were then used to extract metrics.

4.1.2. Extracting an Appropriate Channel Network

Connectivity with the stream was one of the main patch metrics of interest. Deriving an appropriate stream channel network is, however, very difficult in this type of environment. Many of the headwater streams in the Bleaklow area occur in gullies. Most traditional stream extraction methods, particularly those based on simulating channel initiation, assume that network extent (i.e. channel head locations) can be determined using empirical relationships involving contributing area and/or slope. It is difficult to predict channel head locations using these relationships in peatlands. Peatland gullies typically form on gentle slopes. Furthermore, peatland gully heads are often located very near divides and their locations can reflect pre-genetic conditions (i.e. micro topography before the gully formed) rather than a contemporary quasi-equilibrium state. Thus, traditional methods of channel network extraction tend to either underestimate the drainage density in the headwaters of peatland catchments in the Bleaklow region, or to overestimate channel density in parts lower in the catchment (Lindsay and Evans, 2006). That is, it can be very challenging to find an appropriate threshold in upslope area and/or slope to accurately represent channel structures in these environments. As such, an alternative approach was developed based on morphological definition.

The lower quartile (LQ) method (Lindsay, 2006) operates by running a filter over a digital elevation model (DEM). This filter calculates the percentile value of the centre cell with respect to the distribution of elevations within the filter window. The LQ calculations were based on a 2 m LiDAR DEM (section 2.1). A 50 m diameter circular window was used to calculate percentile. Clearly, however, the appropriateness of the selected window diameter depends on the grid resolution relative to the scale of topographic features. Grid cells that were within the lower quartile of the distribution of elevations of their neighbourhood were flagged. Thus, the algorithm identified grid cells that were in relatively low local topographic positions. Unlike most other morphologically-based channel extraction algorithms, the LQ technique avoids defining local minima in 'v'-shaped topographic profiles, which can be a problematic exercise. Nonetheless, this approach to channel mapping is only appropriate in fluvial landscapes. In regions containing numerous lakes and wetlands, the algorithm will pick out the edges of features.

Disjoint channel segments resulting from the thresholding of the percentile image in the above procedure were connected using a flow-tracing algorithm. TAS' *drainage path analysis* algorithm follows the flow path from source cells (i.e. all channel segments) until another non-background grid cell is encountered. This yielded a continuous, unbroken

network of channels. Because it is generally desirable to have single-cell wide channel networks for terrain analysis, the network was post-processed using the line-thinning algorithm available in TAS. The 2 m resolution channel network grid was then resampled, using a nearest neighbour resampling algorithm, to match the resolution of the class image (0.5 m).

Figure 4.3 shows the resulting single-cell wide, continuous channel network for a sub-section of Torside catchment. The algorithm did an excellent job of distinguishing between the high drainage density of the intensively gullied headwaters and the lower channel density in the lower parts of the catchment.

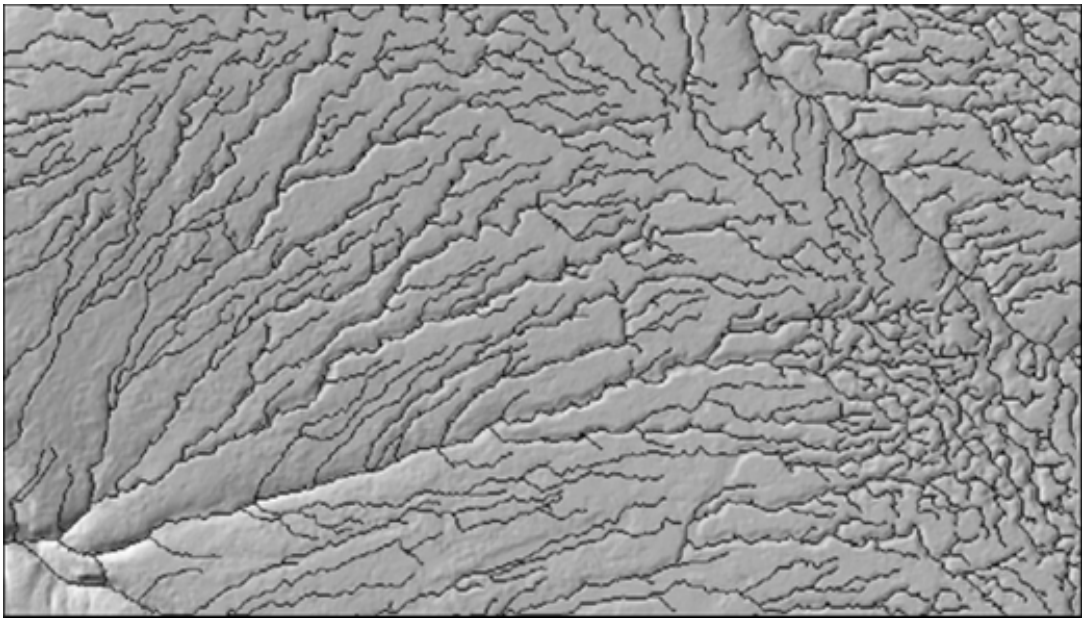

Figure 4.3. Channel network extracted for part of Torside catchment using the LQ method.

4.1.3. Selection of Metrics

A GIS can be used to extract numerous patch metrics. In fact, there are at least 19 common landscape ecology patch metrics used to describe shape alone (McGarigal and Marks, 1995). It can be tempting to extract a suite of metrics to enter into a statistical analysis; however, this approach is inappropriate. Patch metrics are often highly correlated because they are frequently derived from the same base metrics (e.g. area, perimeter, length, etc.). Since the reliability of many statistical models is severely compromised by the increased number of and correlation among predictor variables, it is wise to be parsimonious with the selection of variables.

Ten metrics were extracted for each patch in the Torside and UNG images (Table 4.2). Each metric describes a characteristic of the patch with respect to the land cover, shape (i.e. morphometric), topography, or connectivity with the stream. Topography-type metrics were calculated by extracting information about the terrain within the area of each patch.

Terrain characteristics were based on the 2 m LiDAR DEM. TAS' *descriptive statistics* module was used to create text files for each of the terrain metrics, which could then be easily imported into an Excel spreadsheet. E_{min} and E_{max} were extracted as intermediate

metrics to calculate patch relief (*R*), which was calculated in the spreadsheet rather than extracting it directly in the GIS. Slope (measured in degrees) was calculated for the entire DEM using the available algorithm in TAS and extracted at a patch average level. Maximum flow length was calculated using the *downslope flow-path length* (a.k.a. *distance to outlet*) algorithm. This required using the patch ID image as a mask.

Connectivity was calculated by evaluating the maximum value in the stream channel image to occur in each patch. Thus, if a patch is connected to the stream network it would have a maximum value of 1 (connected), else it would have a value of 0 (disconnected). Again, this can be easily calculated and converted to a text file by using TAS' *descriptive statistics* module.

Table 4.2: List of measured patch metrics.

Metric Type	Metric Name (units)	Symbol	Variable	Description
Land Cover	Patch type		Class_ID	Describes whether the patch is peat (1), mineral soil (2) or vegetation (3)
Morphometric	Area (m^2)	*A*	*Area_m2*	Patch area
	Perimeter (m)	*P*	*Perim*	Patch perimeter
	Shape index	*S*	*Shapeind*	Perimeter / Area
Topography	Minimum elevation (m)	E_{min}	*Min_elev*	Minimum elevation in a patch
	Maximum elevation (m)	E_{max}	*Max_elev*	Maximum elevation in a patch
	Patch relief (m)	*R*	*Max_rel*	*Maximum minus maximum elevation*
	Average slope (degrees)	S_{avg}	*Avgslope*	Average slope of patch
	Maximum flow length (m)	L_{max}	*Max_flow*	Maximum flow path length running though a patch
Connectivity	Connectivity with the stream	*C*	*Connect*	Boolean variable: true (connected, 1) or false (unconnected, 0), indicating whether a stream runs through a patch

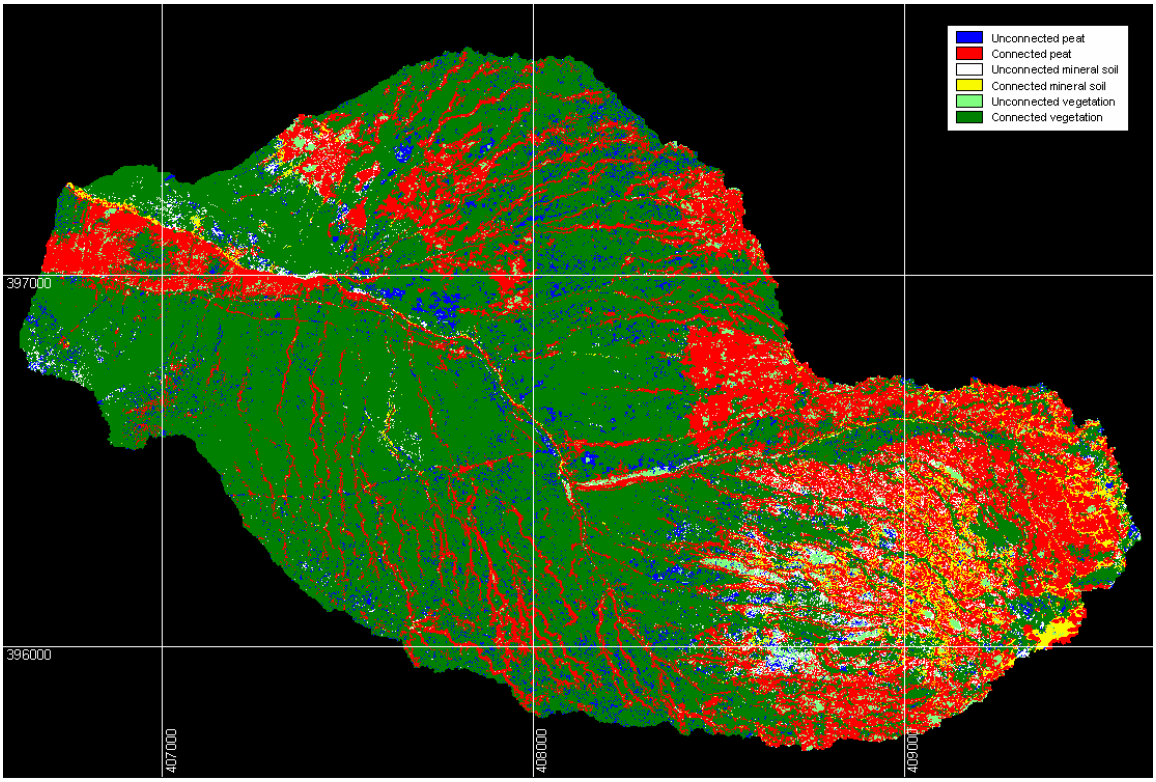

Figure 4.4: Connectivity map for TS with 1 km grid

Each of the metrics in Table 4.2 can be theorised to have a potential impact on the erosive potential of a patch. It is envisioned that, aside from patch type which will clearly have a very significant impact on patch erosion, the topography and connectivity patch metrics will be most important at controlling erosion. Therefore, a connectivity map was produced for each catchment by cross-tabulating connectivity against land cover class[3] (Figures. 4.4 and 4.5). The most significant patches are likely to be connected peat, shown as red. Interpretation of the connectivity images is covered in section 5.2.4.

[3] This was done in TAS but it can be done with other GIS such as MapInfo or ArcGIS using the database provided. Note that the outlet point used to define the UNG catchment here was actually 100m downstream of the gauging station, as used to define it in section 3. This explains the difference in catchment shape.

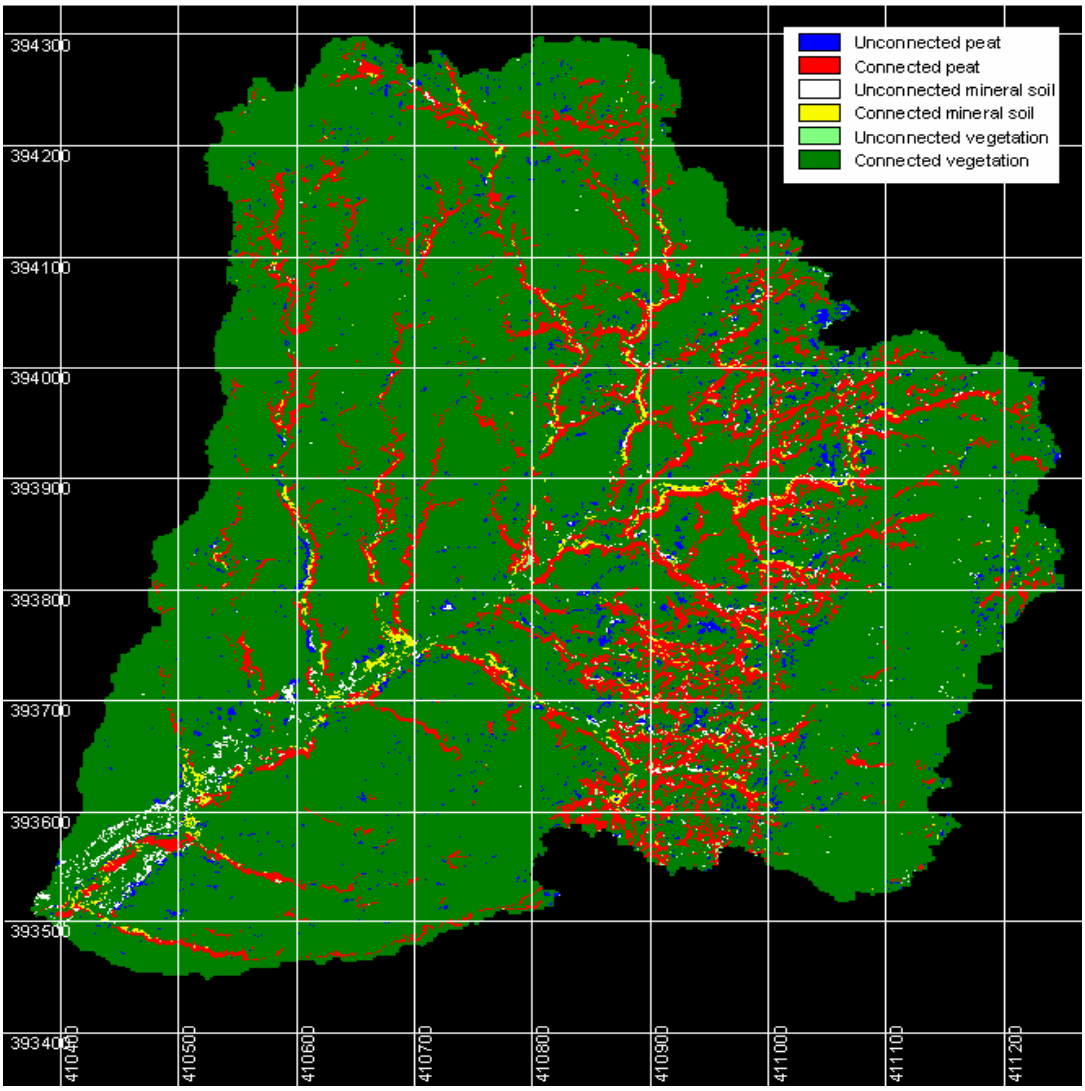

Figure 4.5: Connectivity map for UNG with 100m grid.

4.2. Discussion

Several new algorithms and procedures needed to be developed to perform the metric extraction on the class image. In particular, this work has relied heavily on specialized software, TAS GIS, which was modified to facilitate this research. TAS is a free software package that is easily available to anyone who would wish to replicate this method in the future.

Some important considerations must be made however. First, the quality of the image classification and the characteristics of the landscape itself greatly impact the extraction of patch metrics. If the class image contains numerous small patches, perhaps due to error, simplification of the image must be performed. In this report, we have recommended the use of a sieving procedure for reducing the number of 'irrelevant' patches. This procedure is highly effective and does not corrupt the quality of larger patches. However, the dominant neighbour algorithm described above is slow-running and can act as a bottle-neck in the processing of patch metrics. This fact, combined with

the difficulty of analysing extremely large databases, will place a practical limit on the size of catchment that can be processed (section 6.1).

In this work we have extracted patch metrics for two catchments within the Peak District National Park. Catchments are defined by the area draining to a point. The size of the catchment is extremely dependent on the location of these outlet points. In our case, the outlet points defining our catchments of interest were located because of available discharge data (i.e. the location of monitoring stations). However, there is no reason why future work involving this method of metric extraction could not be applied to catchments that are defined using other methods. For example, it might be useful to consider the sub-catchments of a stream network (i.e. the areas draining each link in the network) or to compare catchments of a similar Strahler stream order. However, since the procedure is limited by the number of patches that can be practically analysed, a logical basis for defining catchments might be catchment area. Lindsay *et al.* (2006) describe a simple method, called the isobasin method, of defining multiple catchments of a specified area. This may also serve as a useful approach for further sub-dividing larger catchments into smaller sub-catchments in order to evaluate the within-catchment variability in peat patch characteristics.

The selection of appropriate patch metrics is imperative to this work. In particular, it is important to consider: (i) the relevance of a metric to the processes involved in peat erosion, (ii) the ease with which a metric can be calculated, (iii) the number of metrics that can be reasonably entered into a statistical model, and (iv) the redundancy of metrics that are derived using similar base metrics.

Not all of the ten patch metrics in Table 4.2 are necessary for the statistical analyses (section 5). Minimum and maximum elevation are intermediate metrics used to evaluate patch relief, and have no physical importance themselves. Patch relief and average slope are both measures of the potential energy available for erosive processes within a patch, so that both are not required in the analysis. Maximum flow length is related to maximum distance that eroded peat must travel over a patch before entering either the stream or a neighbouring patch. This can be seen in two ways; either as implying a long transit time, so of less importance to erosion, or as offering a greater opportunity to entrain sediment by surface wash or creep.

Connectivity with the stream is probably the most useful metric for the erosive potential of a patch, perhaps in combination with slope, area and flow length. Connectivity is, however, extremely dependent on the quality of the channel network that is used to determine connectivity, in particular the ability to accurately represent network extent. It was recommended that traditional methods for extracting channel networks from DEMs do not work well in peatland environments. Instead, a morphologically based method, which identifies areas of low topographic position, is advocated here.

5 STATISTICAL AND SPATIAL ANALYSIS

5.1 Methods

5.1.1 Importing into SPSS

The Excel files for Torside (TS) and Upper North Grain (UNG) were imported separately into SPSS ©. A third file of peat patches from both catchments was produced to enable comparative tests to be carried out. The first variable in each file was patch ID, so that results could be related back to spatial position in TAS. This enabled map outputs to be produced from new variables generated in SPSS.

5.1.2 Generating descriptive statistics

The three nominal variables, connectivity (unconnected, connected), patch type (peat, mineral, vegetation) and catchment (UNG, TS) were used to select subsets of the data. Descriptive statistics for five key quantitative metrics (Area_m2, Shapeind, Max_rel, Max_flow and Avgslope) were calculated for these subsets with SPSS EXPLORE function, and used to compare between and within catchments for different patch types and connectivity. For instance, means and standard deviations of connected peat patches at TS were compared to those at UNG (between catchment comparison), and connected and unconnected peat patches were compared for TS (within catchment comparison). Analysis concentrated on connected peat patches because coupling of bare peat slopes with channels is associated with higher sediment yield (Evans and Warburton, 2005; Evans *et al.,* 2006 in press) and, therefore, greater erosion risk.

5.1.3 Comparing groups

Analysis of variance (ANOVA) was used to test whether variation in the characteristics if patches was significantly greater than variation within them; for instance, if area or average slope of connected peat patches varied more between catchments than within them.

Student's t-test was used to ascertain if differences between metrics were significantly different for catchments or types of patches.

5.1.4 Erosion risk maps

As an example of the type of modeling that can be done using the metrics database, new potential erosion risk metrics were computed. Several combinations of metrics and different ways of combining them were tried. Two variants using Area_m2 and Avgslope are presented here. These metrics were selected following the rationale explained in section 4.1.3 and because they were not co-correlated, but others combinations are valid.

Errisk2 showed *relative* risk within a catchment and was produced by first dividing Area_m2 and Avgslope separately into ten percentile classes using the SPSS CATEGORISE function. The resulting new variables, AREA10 and SLOPE10, were then summed and divided by two to produce risk score ranging from 1-10 in each catchment.

Errisk4 showed risk *between* catchments. Area_m2 and Avgslope were scaled from 1-10, where 1 was the global minimum value over both catchments, and 10 was the global maximum. Clearly, if the technique were extended to other areas of the National Park, new global minimum and maximum values would need to be calculated. Obvious

outliers such as the large patch at TS, which is actually shadow, could be omitted at this stage if all of them are known. The two scaled metrics, SC_AREA and SC_SLOPE, were added and multiplied by 100/2 to scale the data. The final output range was 0 to 61.9, which was then reclassed into 16 equal classes from 0 to 64. The advantage over ERRISK2is that scaling enables values to be compared between catchments as well as within them, but real numbers are produced which require more storage space.

The new Errisk2 and Errisk4 metrics and Patch_ID were exported back into TAS for display as two potential erosion risk maps for each catchment. They can be displayed as continuous grey-scale images or reclassed into classes as required (Figure 5.5 and 5.6). Classes need not be equal; the digital data supplied can be sliced to identify the top 10 percentile if resources only allow the highest priority patches to be treated. The map can be produced directly in most standard GIS packages containing a raster calculator.

5.2 Results[4]

5.2.1 Comparison of erosion status between catchments

Does the relative area of peat, mineral soil and vegetation vary between TS and UNG?

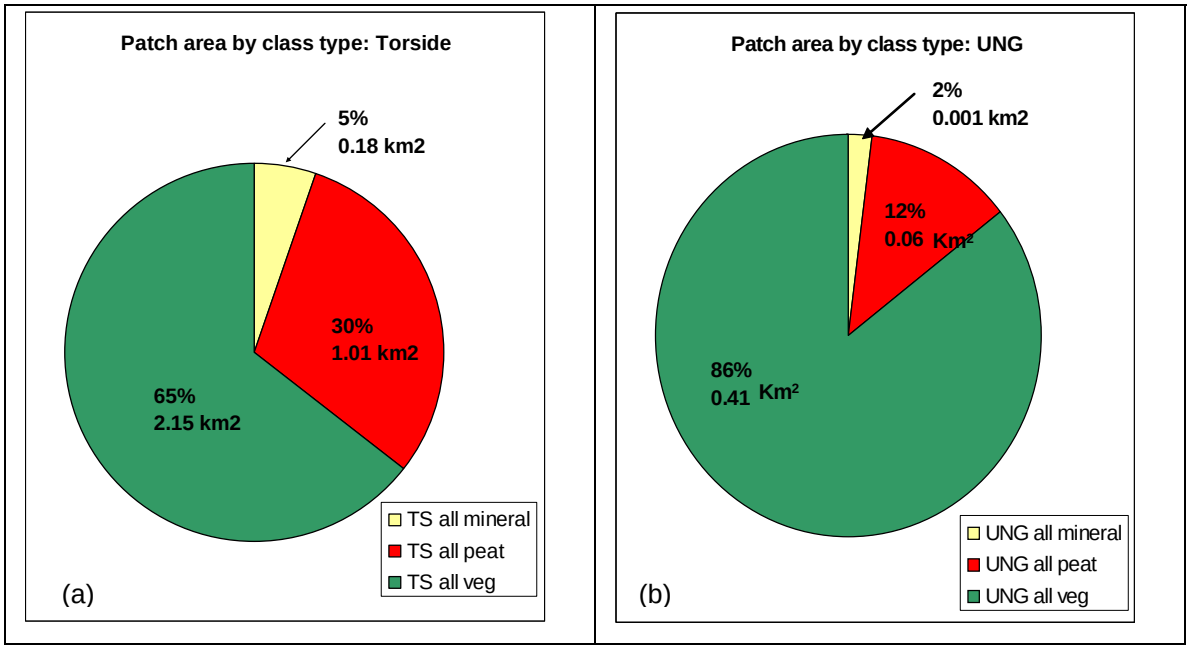

Figure 5.1 (a) and (b): Comparison of patch area by class at TS and UNG

A higher proportion of the area at TS was exposed peat and mineral soil (Figure. 5.1(a) and (b); Tables 5.1(a) and (b)). Thirty percent at TS is (was) peat compared to 12% at UNG. Equivalent values for mineral soils are 5% and 2%. However, the difference between catchments was not as marked as these figures suggest when the greater

[4] The analysis is largely based on patches as classified, including misclassifications, as the intention was to see how well automated methods based on accessible data sources would perform.

misclassification due to shadow at TS is taken into account. For instance, when the third largest patch at TS (shadowed vegetation misclassified as peat) was excluded, peat coverage fell from 30% to 28%. Even so, TS was still at a more advanced stage of erosion in terms of exposed peat and mineral sol area. This may be related to the greater frequency of wildfires at TS, at least, since 1976 (McMorrow *et al*., 2006), possibly associated with the easier access afforded by the Pennine Way, and by the greater cover of more flammable dwarf shrub heath and dry bog relative to UNG. Fires act as triggers to vegetation removal.

Table 5.1(a): Descriptive statistics for key metrics for all mineral soil, peat and vegetation patches at TS.

TS all mineral	**Sum**	**Mean**	**Min**	**Max**	**Std Deviation**	**Median**
Area (m^2)	179037	7.95	0.25	4895.50	63.27	2.25
Shape Index)		4.35	0.44	8.00	1.11	4.33
Max Flowlength (m)		1.52	0.00	100.55	1.74	1.00
Max Relief (m)		0.60	0.00	43.13	0.96	0.37
Average Slope (º)		11.05	0.00	60.95	7.88	9.11
TS all peat						
Area (m^2)	1005199	35.57	0.25	288098.00	1900.27	2.50
Shape Index		3.84	0.31	8.00	1.19	4.00
Max Flowlength (m)		2.02	0.00	234.57	3.99	1.21
Max Relief (m)		0.64	0.00	223.30	2.36	0.32
Average Slope (º)		9.72	0.00	65.99	7.80	7.48
TS all veg						
Area (m^2)	2145060	188.78	0.25	1077757.50	12240.14	3.00
Shape Index		3.51	0.35	8.00	1.28	3.50
Max Flowlength (m)		2.58	0.00	379.43	5.98	1.50
Average Slope (º)		13.37	0.00	61.93	10.05	10.07

Table 5.1(b): Descriptive statistics for key metrics for all mineral soil, peat and vegetation patches at UNG.

UNG all mineral	**Sum**	**Mean**	**Min**	**Max**	**Std Deviation**	**Median**
Area (m^2)	9914	5.16	0.25	210.00	11.71	2.25
Shape Index)		4.17	1.30	8.00	1.18	4.00
Max Flowlength (m)		1.55	0.00	18.12	1.37	1.21
Max Relief (m)		0.71	0.00	8.95	0.89	0.44
Average Slope (º)		13.36	0.01	43.23	8.43	11.62
UNG all peat						
Area (m^2)	59690	21.99	0.25	3995.75	140.85	3.25
Shape Index		3.48	0.80	8.00	1.23	3.50
Max Flowlength (m)		2.47	0.00	34.00	3.21	1.50
Average Slope (º)		9.65	0.00	40.40	6.27	8.42
UNG all veg						
Area (m^2)	414357	835.40	1.25	409141.00	18370.58	2.25
Shape Index		3.52	0.30	6.70	1.13	3.50
Max Flowlength (m)		2.54	0.00	268.99	12.24	1.21
Average Slope (º)		13.21	0.65	40.27	6.71	12.21

Do proportions of connected patches of all types vary between UNG and TS?

It is not simply the area of exposed peat which is important. Connected peat patches present a greater erosion risk. The majority of connected patches in both catchments were vegetation, but a higher proportion were peat at TS than at UNG; 28% compared to 11% (Figure 5.2 (a) and (b); Table 5.2 (a) and (b). Even allowing for the 71103 m^2 misclassified patch, over a quarter of the TS catchment (26%) was at high risk. It should be stressed that this represents the situation pre-restoration, since re-seeded peat and geojute have been recoded to peat.

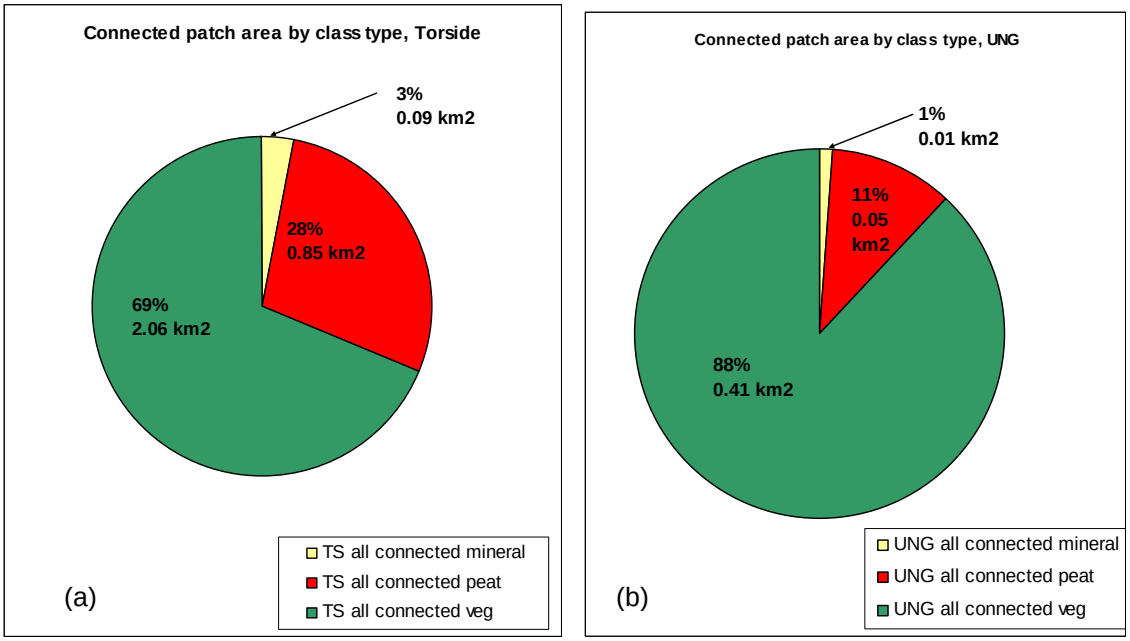

Figure 5.2 (a) and (b): Comparison of patch area by class at TS and UNG for connected patches only

Table 5.2(a): Descriptive statistics for key metrics of connected patches of mineral soil, peat and vegetation at TS

TS connected mineral	**Sum**	**Mean**	**Min**	**Max**	**Std Deviation**	**Median**
Area (m^2)	88888	19.97	0.25	4895.50	137.64	3.00
shape Index (P/A)		4.01	0.44	8.00	1.15	4.00
Max Flowlength (m)		2.24	0.00	100.55	3.03	1.50
Average Slope (º)		9.86	0.12	51.42	6.13	8.78
TS connected peat						
Area (m^2)	853623	233.49	0.25	288098.00	5279.34	4.50
Shape Index		3.43	0.31	8.00	1.39	3.43
Max Flowlength (m)		4.17	0.00	234.57	9.67	1.71
Average Slope (º)		10.56	0.50	49.96	6.73	9.39
TS connected veg						
Area (m^2)	2061445	730.23	0.25	1077757.50	24552.30	4.75

Shape Index		3.13	0.35	8.00	1.31	3.11
Max Flowlength (m)		4.36	0.00	379.43	11.15	2.00
Average Slope (º)		11.52	0.00	61.81	7.90	9.65
TS all connected						
Area (m^2)	3003956	274.84	0.25	1077757.50	12847.71	3.75
Shape Index		3.59	0.31	8.00	1.33	3.60
Max Flowlength (m)		3.43	0.00	379.43	8.25	1.71
Average Slope (º)		10.52	0.00	61.81	6.86	9.24

Table 5.2(b): Descriptive statistics for key metrics of connected patches of mineral soil, peat and vegetation at UNG

UNG connected mineral	**Sum**	**Mean**	**Min**	**Max**	**Std Deviation**	**Median**
Area (m^2)	5333	7.23	0.25	210.00	16.37	2.75
Shape Index (P/A)		4.02	1.30	8.00	1.19	4.00
Max Flowlength (m)		1.87	0.00	18.12	1.69	1.50
Average Slope (º)		12.84	0.01	42.58	7.72	11.11
UNG connected peat						
Area (m^2)	50587	56.59	0.25	3995.75	241.42	8.25
Shape Index		2.90	0.80	8.00	1.24	2.70
Max Flowlength (m)		4.21	0.00	34.00	4.70	2.71
Average Slope (º)		11.12	0.00	40.40	6.22	9.99
UNG connected veg						
Area (m^2)	413628	1504.10	1.25	409141.00	24671.25	3.25
Shape Index		3.26	0.30	6.40	1.17	3.30
Max Flowlength (m)		3.49	0.00	268.99	16.36	1.50
Average Slope (º)		12.72	0.71	40.27	6.00	11.81
UNG all connected						
Area (m^2)	469548	246.22	0.25	409141.00	9369.90	4.50
Shape Index		3.38	0.30	8.00	1.32	3.30
Max Flowlength (m)		3.20	0.00	268.99	7.15	1.71
Average Slope (º)		12.02	0.00	42.58	6.86	10.69

To summarise, UNG was a more vegetated, lower risk catchment. The fact that over a third (35%) of the TS catchment was unvegetated compared to 14% at UNG suggests that erosion at TS is at more advanced stage than at UNG. Over a quarter (28%) of the connected patches were peat, compared to only 11% at UNG, so potential erosion risk was greater at TS.

5.2.2 Within-catchment variation in erosion status

Do proportions of peat, mineral soil and vegetation vary within TS, and within UNG?

The same 6:1 ratio of peat to mineral soil area is (was) found at both catchments (Figure 5.1 (a) and (b); Table 5.1 (a) and (b).

Do proportions of connected to unconnected peat vary within TS, and within UNG?

If the area of connected and unconnected peat patches is compared, the same proportion was found for TS and UNG (85%) (Figure. 5.3(a); Table 5.3). The fact that majority of peat area was connected to the channel represented high potential erosion risk at both.

In terms of the number of peat patches, unconnected patches were more dominant than connected ones at TS (87; 13%) than they were at UNG (67:33%) (Figure 5.3(b); Table 5.3).

Both observations would seem to suggest that erosion risk in the two catchments is equal. However, it is the *connected* patches which are critical, and their relative and absolute area were greater at TS (section 5.2.1) as is also obvious from the larger area of red on Figures 4.4 compared to Figure 4.5. Relative sizes and other characteristics of individual patches will be explored next.

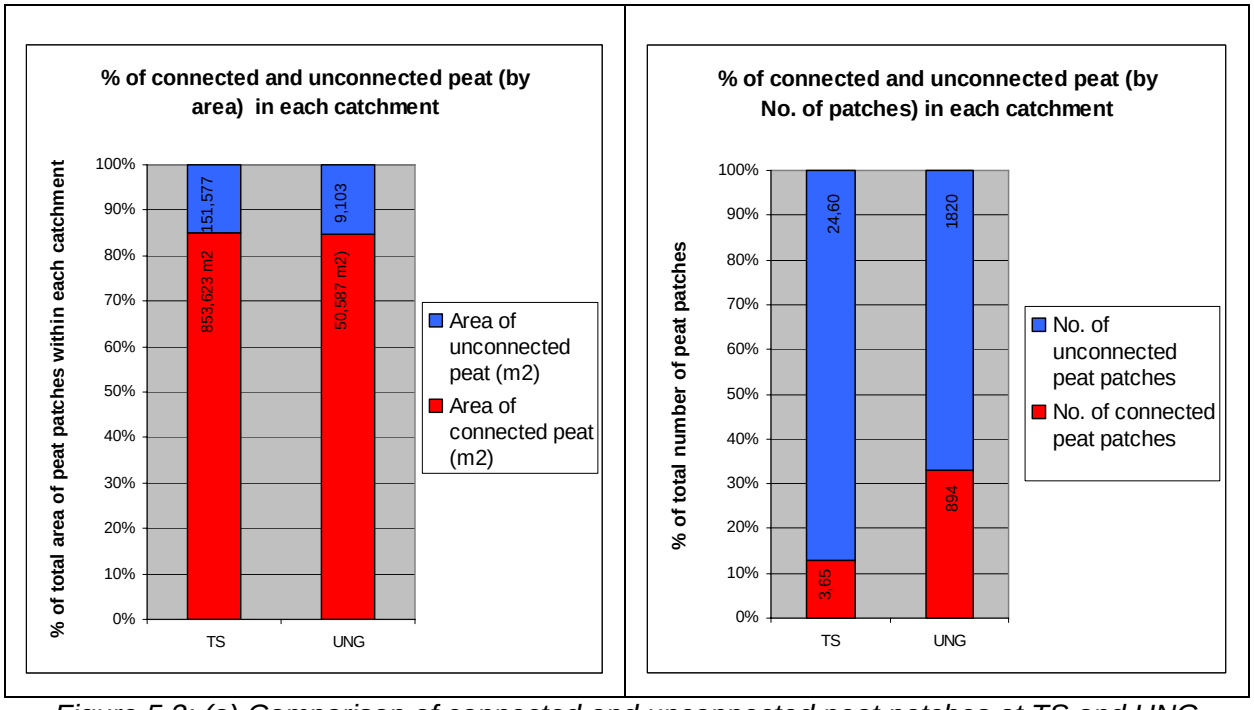

Figure 5.3: (a) Comparison of connected and unconnected peat patches at TS and UNG by area, (b) Comparison of connected and unconnected peat patches at TS and UNG by number.

Table 5.3: Area and number of connected and unconnected peat at TS and UNG.

	TS	UNG
Area of connected peat (m^2)	853623 [85%]	50587 [85%]
Area of unconnected peat (m^2)	151577 [15%]	9103 [15%]
No. of connected peat patches	3656 [13%]	894 [33%]
No. of unconnected peat patches	24606 [87%]	1820 [67%]

5.2.3 Characteristics of connected peat patches

Do metrics for connected peat vary significantly between UNG and TS?

Parameters for the four metrics discussed below are given in Tables 5.2(a) and (b). The t-test showed that mean patch size at TS (233 m^2) was significantly larger than at UNG (57 m^2) (p 0.044). However, both TS and UNG had very skewed distributions with a few very large patches, so the median is a better comparative measure, and TS patch median was, in fact, half that of UNG (4.5, 8.25 m^2).

Connected peat patches at TS were significantly less compact than UNG, and had shorter but more variable flow lengths. They were also flatter (p 0.012) with modal value 8 degrees at TS and 10 degrees at UNG, and both average slope distributions were positively skewed.

However, ANOVA showed that there was significantly more variation between catchments than within them only for two metrics: shape and average slope (p 0.000, 0.025).

Is there greater variation in key metrics of peat patches between unconnected and connected patches (for both catchments combined) than within these two groups?

Connected peat patches were larger but more variable in size, more compact, longer but more variable in flow length, and flatter but with more variable relief. (Table 5.4). ANOVA showed that there was significantly more variation between the two connectivity classes than with them for all four metrics (p 0.000) (Table 5.5).

Table 5.4: Descriptive statistics for all unconnected peat patches (TS and UNG) compared to all unconnected peat patches.

Total unconnected peat N = 26426					
	Mean	**Std. Deviation**	**Minimum**	**Maximum**	**Median**
Area (m^2)	6.08	25.01	0.25	1737.00	2.25
Shape Index (P/A)	3.89	1.14	0.51	8.00	4.00
Max Flowlength (m)	1.69	1.87	0.00	62.37	1.21
Average Slope(º)	9.55	7.84	0.00	65.99	7.28
Total connected peat N = 4550					
Area (m^2)	198.73	4733.95	0.25	288098.00	5.00
Shape Index (P/A)	3.33	1.38	0.31	8.00	3.27
Max Flowlength	4.17	8.92	0.00	234.57	2.00
Average Slope	10.67	6.64	0.00	49.96	9.51

Table 5.5: ANOVA for total connected versus total unconnected peat.

		Sum of Squares	df	Mean Square	F	Sig.
Area (m^2)	Between Groups	144059525	1	144059524.69	43.76	0.000
	Within Groups	101960981630	30974	3291824.81		
	Total	102105041154	30975			
Shape Index (P/A)	Between Groups	1234	1	1234.09	883.66	0.000
	Within Groups	43257	30974	1.40		
	Total	44491	30975			
Max Flowlength (m)	Between Groups	23950	1	23950.49	1634.26	0.000
	Within Groups	453933	30974	14.66		
	Total	477883	30975			
Average Slope	Between Groups	4871	1	4871.24	82.75	0.000
	Within Groups	1823272	30974	58.86		
	Total	1828143	30975			

Further analysis could focus on which metrics best discriminate between connected and unconnected peat patches. Discriminant function analysis can be used to identify which metrics best discriminate between connected and unconnected patches. Work so far suggests that maximum flow is an important discriminator, as might be expected for connected patches. Similarly, factor analysis can be used to derive a new combined metric for connected peat patches, based on a weighted combination of the original metrics.

Cluster analysis can be carried out on connected peat patches for each catchment. Patches are grouped by the similarity of their metrics, or factors from factor analysis, and then mapped to see if the clusters have a particular spatial distribution. For instance, are some clusters restricted to certain aspects or peat depths?

5.2.4 Analysis of connectivity maps

How does connectivity vary within between and within TS and UNG?

The connectivity maps produced in section 4 (Figures 4.4 and 4.5), confirm the statistical results. A greater degree of slope-channel coupling in exposed peat is seen at TS (prior to reseeding) than at UNG. The large horizontal Y-shaped peat flat on Sykes Moor, smaller flats at Torside Grain and much of Joseph's Patch emerge as connected peat patches and justify the restoration work that has already been carried out (Figure 5.4). Shining Clough stands out as a priority for reseeding, as almost all the peat in this area is connected to channels

Advanced Bower type 1 stage of erosion (Bower, 1960, 1961) is seen at Bleaklow Head where a large patch of connected mineral soil surrounds connected peat. Some misclassification is obvious, especially in Joseph's Patch, where recently burns have been misclassified as mineral soil. The Pennine Way north of Bleaklow Head is correctly classified as connected mineral soil (yellow), because the path is also identified from the DEM as a channel. Indeed, overlaying the wayline data on the channel network or connectivity map would show how much connectivity is due to the path network doubling as channels.

At UNG, the connectivity map (Figure. 4.5) shows that a north-south strip to the east of the centre is the most degraded pat of the catchment, as evidenced by amount of mineral soil and peat exposed. It is also the highest risk area because most of the

connected peat is found here. Elsewhere the patches are much more linear than TS, occurring along gullies (Bower type 2). There are few extensive connected peat flats, perhaps because fewer wildfires have occurred here in the last 30 years.

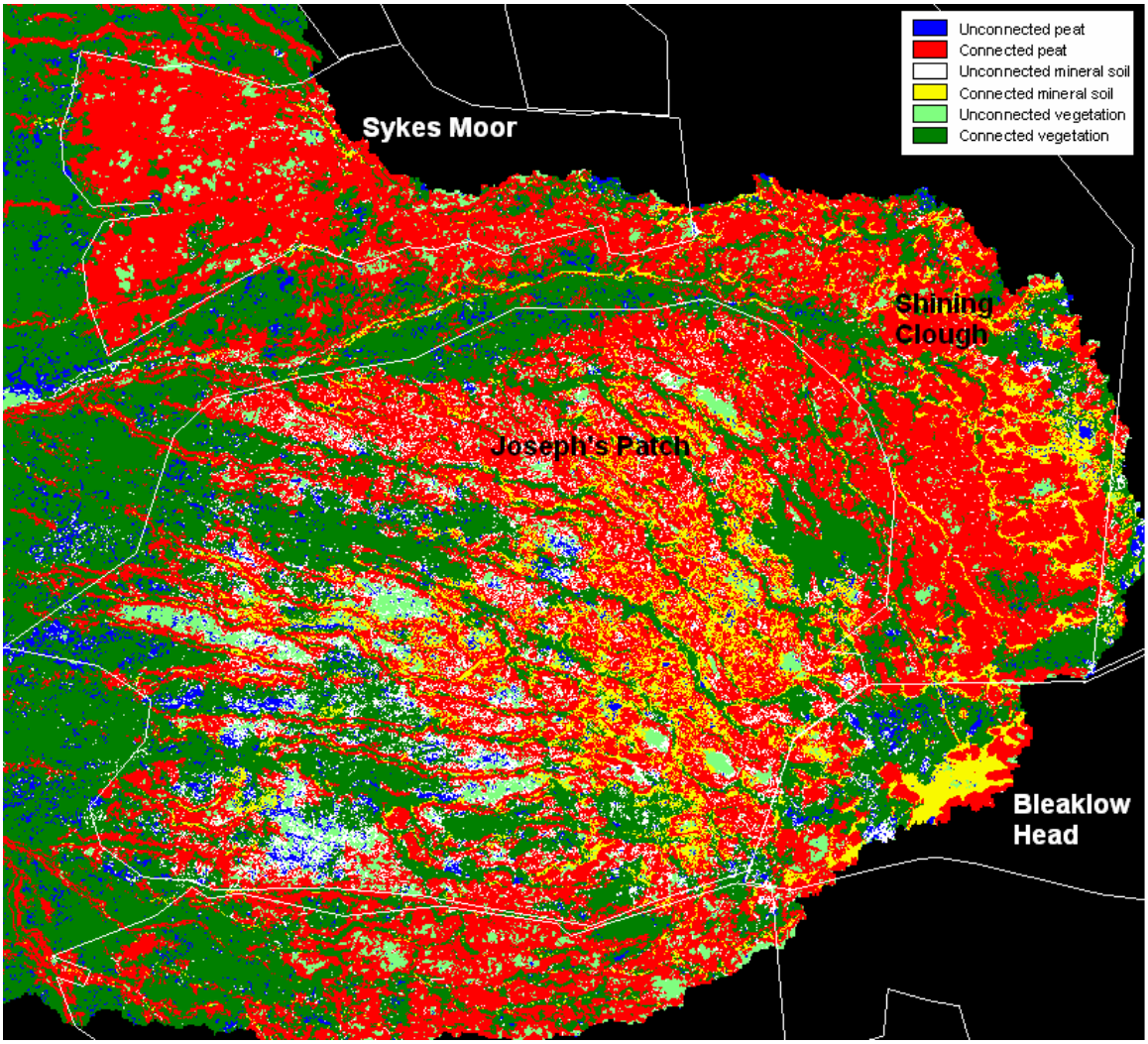

Figure 5.4: Extract from Figure 4.4 connectivity map for the SE part of the TS catchment, showing pre-restoration situation. Reseeded areas are overlaid as white polygons. Red areas are most at risk. Shining Clough emerges as a priority for reseeding.

5.2.5 Analysis of erosion risk maps

How does erosion risk vary within catchments?

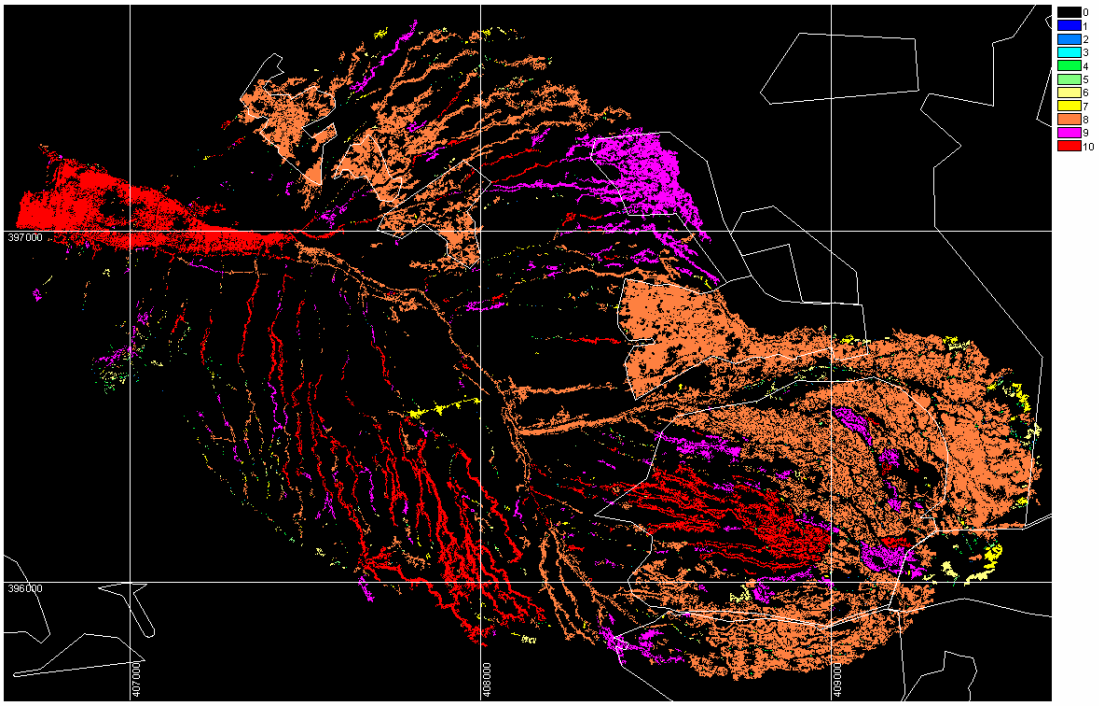

Figure 5.5: ERRISK2 for TS with 1 km grid. Reseeded areas shown as white polygons.

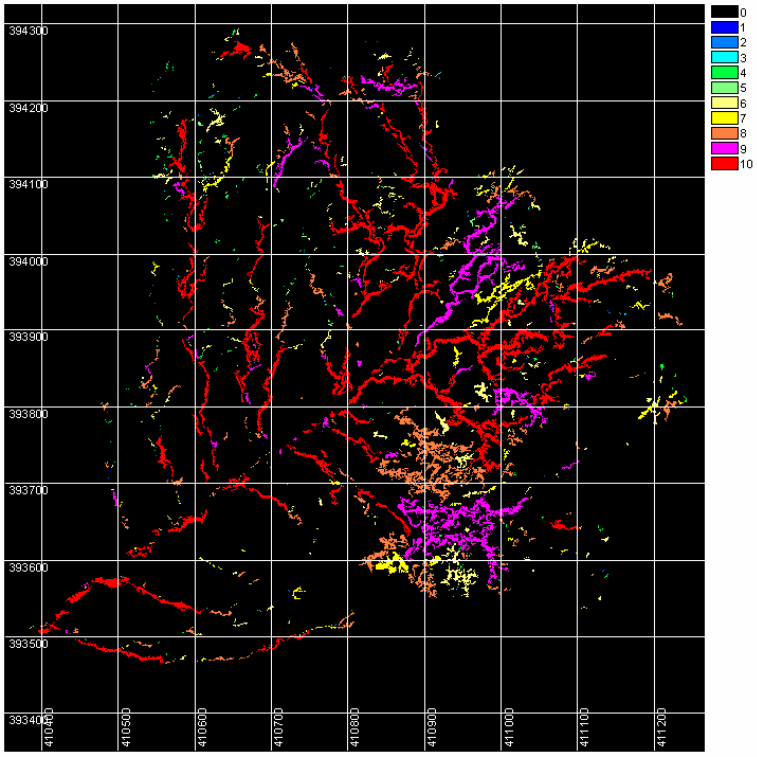

Figure 5.6: ERRISK2 for UNG with 100m grid.

Red and magenta tones on the ERRISK2 maps (Figures 5.5 and 5.6) show the largest, steep connected peat patches. Most of these are already being treated at TS. The red patch on TS Clough is shadow not peat. At UNG, the high risk patches are much more linear and associated with gullies, so gully blocking may be a better option than reseeding.

How does erosion risk vary between catchments?

It is only valid to compare catchments using ERISK4. Unexpectedly, the means was actually higher for UNG (11.1 compared to 10.6). However, the distributions are positively skewed, affected by the few large patches. When the modes are compared TS is higher (Figures. 5.7(a) and (b)). Greater overall risk is suggested at TS when Figures 5.8 and 5.9 are compared.

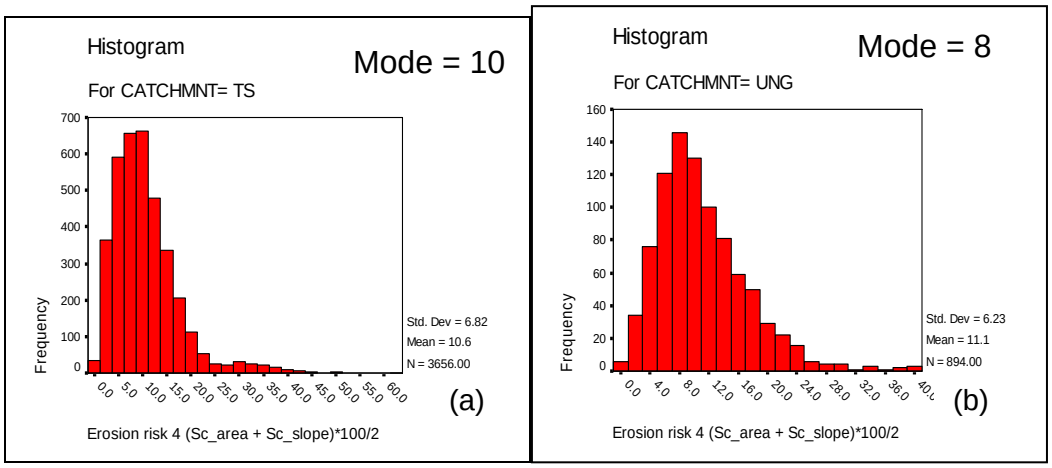

Figure 5.7: Histograms of ERRISK4 for (a) TS and (b) UNG.

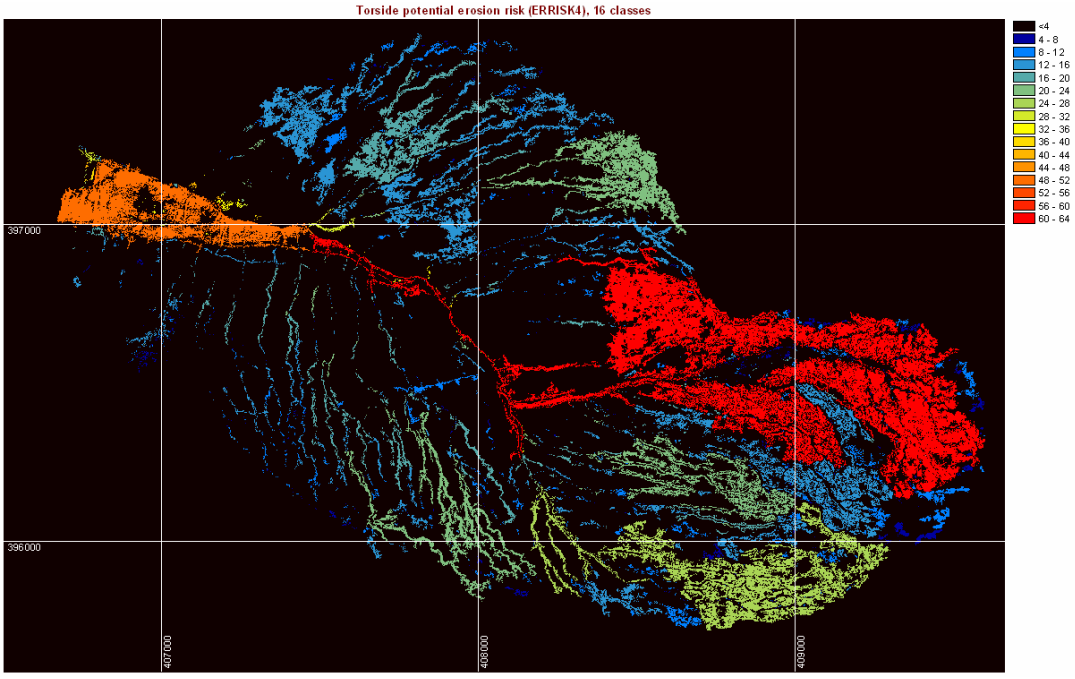

Figure 5.8: TS potential erosion risk (ERRISK4), 16 equal classes

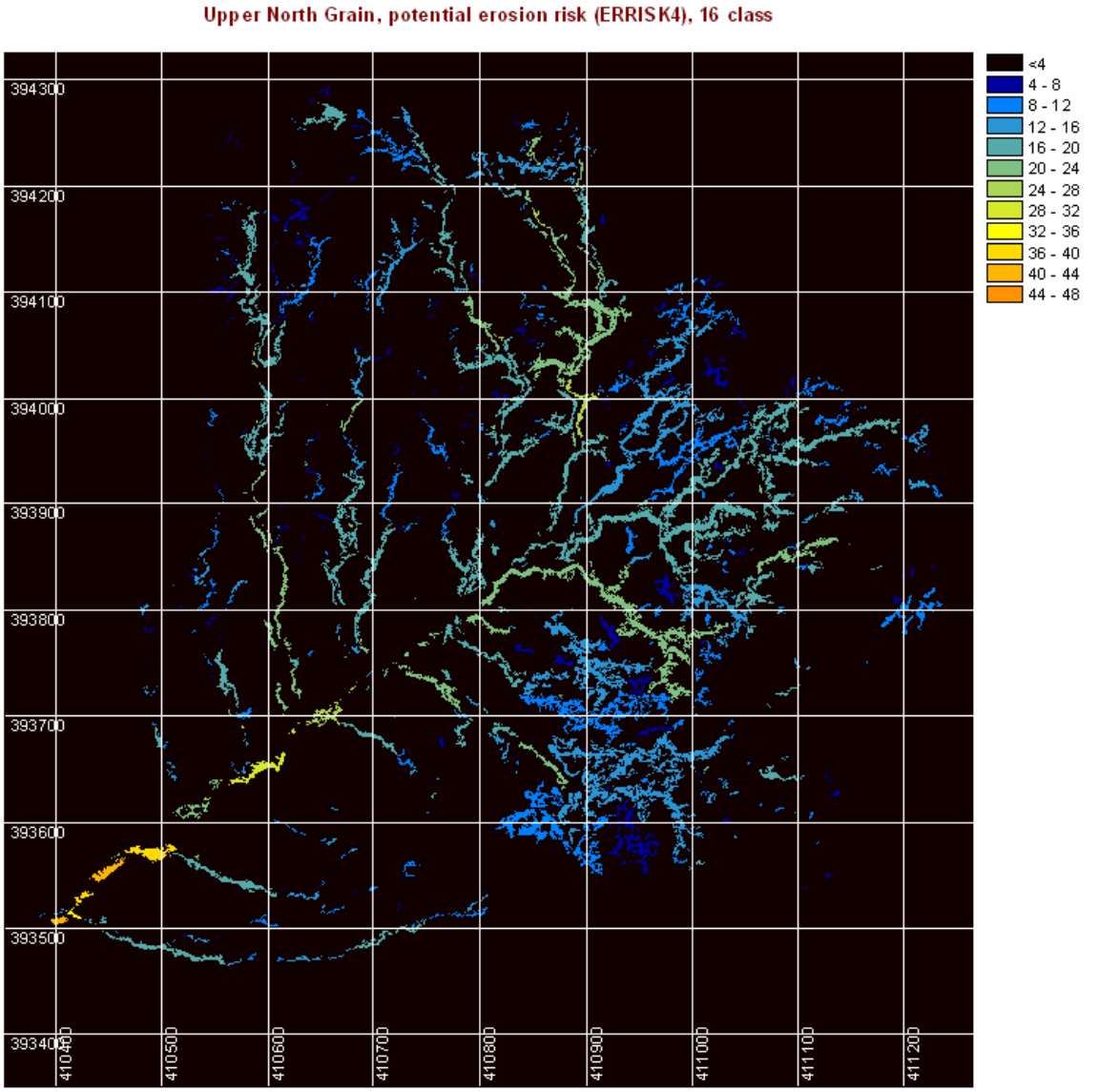

Figure 5.9: UNG potential erosion risk (ERRISK4), 16 classes

5.3 Discussion and recommendations

5.3.1 Extracted metrics

Significant differences emerged between the landscape compositions of the two catchments. TS was the more degraded, with a larger relative and absolute area of exposed peat and mineral soil patches than UNG. It also had a larger area of connected peat patches, so that connectivity of critical patches and potential erosion risk was greater for TS. Restoration measures have already been concentrated here.

Means and distributions were skewed by a few large misclassified patches, which need to be screened out. However, there is genuine tail of a few very large patches with many more smaller ones, especially at TS. The largest are the peat flats at here created by fire.

The significant differences found in the metrics between connected and unconnected peat patches, suggest that it may be possible to recognise connectivity from their larger size, more compact shape, longer flow length and less steep slope, but would need to be tested with a larger sample of catchments.

5.3.2 *Connectivity and erosion risk maps*

The connectivity map is a useful guide to pinpoint priority areas for reseeding. In contrast, the trial erosion risk maps are not much less as useful products, partly because they use area and at least one large patch is misclassified.

The risk maps should be regarded as an example of what can be produced from the database. Other risk maps could readily be produced from the database supplied, either using SPSS, Excel, or directly in a GIS such as TAS or MapInfo. More appropriate metrics can be chosen to express the relative degree of risk for connected peat patches, for instance, flow length or shape, and combined in other ways (multiplication, ratios, etc). Practical considerations can also be built in. For instance, patch shape could be incorporated, as a single large compact shape may be easier to locate for helicopter reseeding than several connected linear ones.

Many different styles of maps can be produced from the same digital risk image. For instance, it can be sliced equally to represent 3, 5 or more classes, or just the top 10% highest risk classes could be displayed.

The connectivity and erosion maps presented here, and others maps which may be produced from the database, could be used to guide restoration work. However, there are three important caveats.

(i) The first relates to the assumptions underlying the model. The assumption that connected peat patches at TS and UNG have the highest erosion risk should ideally be tested against field data. Calibration against field data on sediment delivery from patches would provide a way of validating alternative erosion risk models. It would also allow testing of sensitivity to the various factors affecting the quality of the inputs, i.e. the thematic and geometric classification accuracy of the *patch map*; and, similarly, the accuracy and geometry of the *channel network* and *topographic metrics*. The other two caveats relate to the quality of these inputs.

(ii) The risk maps and underlying database require error checking for misclassified patches. Causes of misclassification identified in section 3 include time of day or year (low sun angle creating shadow); time of year (vegetation phenology reducing contrast with mineral soil and peat). Most notably, a very large patch of ‘peat’ at Torside is actually shadow (orange tones on Figure 5.8). Other misclassifications have occurred, for instance, burnt peat is confused with heather, and some reseeded and brash-covered peat with vegetation. Some types of error, such as peat protected by geojute classified as mineral soil, have been reduced using context measures, but others remain. Erroneous connected peat patches, especially those due to shadow, need to be screened out using visual interpretation of the aerial photographs and field knowledge. Ultimately, the identification of peat by multispectral classification is ultimately dependent on the quality of the image data. Images that use the shortwave infrared art of the spectrum or hyperspectral sensors with narrow bands are likely to improve thematic accuracy.

(iii) Connectivity of some patches may not be accurately represented. Connectivity is extremely dependent on the quality of the channel network used to determine connectivity, in particular the ability to accurately represent network extent.

Traditional methods for extracting channel networks from DEMs do not work well in peatland environments. Instead, a more appropriate morphologically based method, which identifies areas of low topographic position, has been advocated in this work. However, connectivity is only as good as the fit between the patch map and the channel network and the issue of geometric error of the patch map remains. So too does the accuracy of the DEM. Slope and other topographic metrics are only as good as the locational and heighting accuracy of the elevation data. Accuracy would improve if the 0.5 m photogrammetric DEM extracted by UKP were used.

Suggestions of further work to improve inputs is identified in section 6.3.

6. CONCLUSION

6.1 Summary of recommendations

1 The LiDAR had good geometric accuracy, but an independent dGPS survey of ground control points should be obtained, against which geometric quality of the LiDAR DEM and aerial photographs can be judged.

2 The UKP-CIR aerial photography had the best thematic and geometric accuracy of the three AP data sets so is the data source recommended for encoding erosion pattern.

3 Its lower spatial resolution (0.5 m) relative to 0.25 m for GM and UKP meant that small patches in gully floors were not detected. Despite this, a finer resolution is not recommended, as 0.5 m produced too many patches to handle without sieving. Furthermore, the added cost of being able to see finer detail cannot be justified if it means using true colour instead of CIR, or not having photos orthorectified. Both thematic and geometric accuracy are vital for erosion risk mapping and for monitoring revegetation.

4 If new aerial photography is flown, it should ideally be: CIR; obtained in summer to maximise spectral contrasts and as close as possible to solar noon to minimise shadow; ortho-rectified to improve fit to LiDAR for connectivity analysis; and not finer than 0.5m spatial resolution unless for small areas (<1 km^2).

5 The pattern analysis method used here requires hard classification, that is, a pixel is forced into a single class. For this purpose, maximum likelihood supervised classification is recommended, but only on unstretched and uncompressed data. Representative spectral signatures developed for one catchment can be applied to others with minor adaptations.

6 As natural and managed revegetation progresses, it will become less appropriate to use hard classification methods. Soft classification methods, such as spectral unmixing, which calculate the probability of membership to peat and vegetation classes, will need to be explored.

7 The size of the image extracts to be classified and encoded should be chosen according to computer specification; for instance, ideally not larger than 0.5 km^2. The outlet points of the catchments used here were gauging stations. In retrospect, the Torside catchment (3.31 km^2) was too big to process easily at 0.5m resolution and with three bands, resulting in classified images of 21.8 Mb per image (allowing for a minimum number of mask pixels outside the catchment boundary). UNG (0.38 km^2) was much more manageable at 2.3 Mb. It is recommended that Torside should be divided into sub-catchments or isobasins (Lindsay *et al.,* 2006, section 4.2) to speed up processing. This would also enable parts of a catchment to be compared and within-catchment spatial variation studied.

6.2 Extent to which objectives were fulfilled

The project has been reasonably successful within the limitations of the data.

- Quality of the data sets has been evaluated and recommendations made (objective 1).
- Six sets of peat, mineral soil and vegetation class maps were produced and evaluated (objective 2) The most appropriate combination of dataset and multispectral classification method was identified, but accuracy was limited by the data sources available (objective 3).
- A database of morphological and topographic metrics has been successfully extracted for two catchments (see attached CD) (objective 4).
- This required a new method to be developed for extracting a suitable channel network from the DEM (provided on the CD), and development of an automated method for extracting metrics. Connectivity metrics were extracted by combining the channel network with a patch map produced from classification (objective 5).
- Basic spatial variations in patch metrics within and between were statistically analysed, although more could be done (objective 6).
- Objective 7 had mixed success. The connectivity map is a useful tool and could be used in conjunction with other digital map data in the MFF database to assist in planning restoration works, with the caveats identified in section 5.3.2. The erosion risk maps were less successful, but there is scope to develop more appropriate models from the data supplied.
- Recommendations for further work are made below (objective 8).

6.3 Further work

6.3.1 Testing connectivity and erosion risk maps

The relationship between mapped potential erosion risk and actual measured erosion should be assessed. This could be achieved by using the connectivity map or perhaps, better erosion risk maps, to locate sampling sites for field monitoring of slope-channel sediment supply and POC in streamflow. Sites could be chosen to represent the range of postulated risk for connected peat patches with paired control sites on unconnected patches. Different models (combinations of metrics) could be tested against the field data.

6.4.2 Sensitivity analysis

Sensitivity of the connectivity and erosion risk maps to factors affecting their inputs should be investigated (patch map, channel network and DEM). Pertinent factors for the patch map include alternative image sources (such CASI, SPECIM and other airborne scanners), use of topographic and other collateral data and alternative classification methods (Figure 2.4). Sensitivity to factors such as sieve threshold could also be explored.

Similarly, sensitivity to factors affecting the connectivity and topographic metrics should be investigated. These include DEM resolution (Cho and Lee, 2001) and method of extracting the channel network (Lindsay, 2006; Heine *et al.* 2004). One would expect

the photogrammetric DEM supplied with the UKP-CIR photos to produce more reliable results, but data volume would be very large.

6.4.3 Further pattern analysis

More complex pattern analysis to assist gully-blocking could be undertaken if thematic and geometric classification accuracy can first be improved; for instance, to answer the question 'Which gullies are most eroded?' This would involve analysis of connected mineral patches from the connectivity map which were also linear (large shape index) and adjacent to linear patches of peat (indicating deep incision of gullies at quite advanced stages of erosion). The TAS flow-tracing algorithm could first be used to merge individual pixels and lines of pixels along channels, prior to sieving and clumping. The map could be combined with gully depth maps produced from the DEM (Lindsay & Evans, 2006) and existing methods (Haycock, 2004) to refine locations for gully-blocking.

A similar method might be used to identify gully floors which are re-vegetating naturally or after gully blocking, and associated with reduced sediment yield (Evans and Warburton, 2005). It should be noted that only mineral-floored and vegetated gullies wider than 1.5 to 2 m are likely to be identified with 0.5m resolution CIR photography. Increasing spatial resolution to 0.25 m would allow mineral soil or vegetation pixels on gully floors to be more easily detected, but there would be a four-fold increase in data volume. Unless, small areas were being analysed, there would be too many patches to handle and cost would increase.

6.4.4 Overview

In summary, further research on mapping and encoding erosion pattern should be directed at:

(i) improving the accuracy of connectivity using the finer resolution DEM supplied with the UKP-CIR photographs;

(ii) improving the accuracy of the simple three-class of peat, mineral soil, vegetation map using remotely sensed data at longer wavelengths and with narrow bands, and ore advanced classification methods;

(iii) quantifying the error for each peat patch.

Beyond pattern, the alternative techniques and data sources suggested should be evaluated for their ability to extract information for monitoring revegetation on treated areas.

7. ACKNOWLEDGEMENTS

This research was conducted with a Moors for the Future Small Project Grant scheme No A79419. We authors gratefully acknowledge the financial support and, especially, the support of the MFF team. Their assistance has been invaluable in providing data sets and information and in liaison with stakeholders.

8. REFERENCES

Belyea, L.R. & J., Lancaster. (2002) Inferring landscape dynamics of bog pools from scaling relationships and spatial patterns. Journal of Ecology, 90, 223-234.

Berberoglu S, Lloyd CD, Atkinson PM and Curran PJ. 2000. The integration of spectral and textural information using neural networks for land cover mapping in the Mediterranean. Computers and Geosciences, 26: 385-396.

Bower MM. 1960. Peat erosion in the Pennines. Advancement of Science, 64: 323 - 331.

Bower MM. 1961 The distribution of erosion in blanket peat bogs in the Pennines. Transactions of the Institution of British Geographers 29: 17-30.

Bragg OM and Tallis, JH. (2001) The sensitivity of peat-covered upland landscapes. Catena, 42, 345-360.

Brown, D. G., Lusch, D. P. & Duda, K. A. 1998. Supervised classification of types of glaciated landscapes using digital elevation data. Geomorphology 21(3-4): 233.

Campbell JB. 2002, Introduction to Remote Sensing. London: Taylor and Francis.

Casals-Carrasco P, Kubo S and Babu Madhavan B. 2000. Application of spectral mixture analysis for terrain evaluation studies. International Journal of Remote Sensing, 21(16): 3039-3055.

Charman D. 2002. Peatlands and Environmental Change. Wiley, Chichester.

Cho SM and Lee M. 2001. Sensitivity considerations when modeling hydrologic processes with digital elevation model. Journal of the American Water Resources Association, 37 (4): 931-934.

Cihlar J, Qinghan Xiao J, Chen J, Beaubiens J, Fung K and Latifovic R. 1998. Classification by progressive generalization: a new automated methodology for remote sensing multichannel data. International Journal of Remote Sensing 19(14): 2685-2704.

Clergeau P and Burel F. 1997. The role of spatio-temporal patch connectivity at the landscape level: an example in a bird distribution. Landscape and Urban Planning, 38: 37-43.

Cutler MEJ, McMorrow JM and Evans MG. 2002. Remote sensing of upland peat erosion in the Southern Pennines. Northwest Geography.2(1): 20-30, [available online, accessed 29 July 2006] http://www.art.man.ac.uk/Geog/mangeogsoc/4_2_1_2002.htm

Dean AM and Smith GM. 2003. An evaluation of per-parcel land cover mapping using maximum likelihood class probabilities. International Journal of Remote Sensing, 24(14): 2905-2920.

Eastman RJ. 2003. IDRISI Kilimanjaro Guide to GIS and Image Processing Clark Labs Clark University: Worcester, MA

Ekstrand S. 1996. Landsat TM-based forest damage assessment: correction for topographic effects. Photogrammetric Engineering and Remote Sensing, 62, 151-161.

Evans MG and Warburton J. 2005. Sediment budget for an eroding peat-moorland catchment in northern England. Earth Surface Processes and Landforms, 30(5): 557-577.

Evans M, Warburton J and Yang J. 2006 in press. Sediment Budgets for Eroding Blanket Peat Catchments: Global and local implications of upland organic sediment budgets. Geomorphology.

Evans M, Allott T, Holden J, Flitcroft C and Bonn A. 2005. Understanding gully blocking in Deep Peat. Moors for the Future Report No 4. Moors for the Future, Castleton. 105pp http://www.moorsforthefuture.org.uk/mftf/downloads/publications/Gully%20Blocking%20report.pdf [Available online, accessed 28 July 2006]

Foody GM. 1996. Approaches to the production and evaluation of fuzzy land cover classifications from remotely sensed data. International Journal of Remote Sensing, 17 (7): 1317-1340.

Foody GM. 2000. Estimation of sub-pixel land cover composition in the presence of untrained classes. Computers and Geosciences, 26: 469-478.

Freeman C, Evans CD, Monteith DT, Reynolds B and Fennerm N. 2001. Export of organic carbon from peat soils. Nature, 412, 785.

Gorham E, 1991, Northern peatlands: role in the carbon cycle and probable responses to climatic warming. Ecological Applications, 1 (2): 182-195.

Haycock N. 2004. Processing of LiDAR data for the identification of critical peat mass areas and delineation of peat gully network – outline nores and methodology. Report for National Trust High Peak Estate and National Trust Cirencester. Haycock Associates Ltd, St Albans. 21pp.

Heine, RA., Lant, CL., and Sengupta, R.R. 2004. Development and comparison of approaches for automated mapping of stream channel networks. Annals of the Association of American Geographers, 94 (3): 477-490.

Holden J. 2005. Peatland hydrology and carbon release: why small-scale process matters Philosophical Transactions of the Royal Society A: Mathematical, Physical and Engineering Sciences 363(1837): 2891-2913.

Holden J, Hobson G, Irvine B, Maxfield E, James T and Brookes C. 2005. Strategic locations for gully blocking in deep peat. In Evans M *et al.* Understanding Gully Blocking in Deep Peat. Moors for the Future Report No 4. Moors for the Future, Castleton. Moors for the Future Castleton, pp 77-95. [available online, accessed 28 July 2006] http://www.moorsforthefuture.org.uk/mftf/downloads/publications/Gully%20Blocking%20report.pdf

Huang C, Davis LS and Townshend JRG. 2002. An assessment of support vector machines for land cover classification. International Journal of Remote Sensing 23(4): 725-749.

Jones AR, Settle JJ and Wyatt BK. 1988. Use of digital terrain data in the interpretation of SPOT-1 HRV multispectral imagery. International Journal of Remote Sensing, 9**:** 669-682.

Keramitsoglou I, Sarimveis H, Kiranoudis CT, Kontoes C, Sifakis N and Fitoka E. 2006. The performance of pixel window algorithms in the classification of habitats using VHSR imagery ISPRS Journal of Photogrammetry and Remote Sensing 60(4): 225-238.

Labadz JC, Burt TP, Potter AWR. 1991. Sediment yield and delivery in the blanket peat moorlands of the Southern Pennines. Earth Surf Process Landforms, 16:255 –271.

Liddaman LC, McMorrow JM and Evans MG. 2004. Eroding blanket peat: utilising pattern analysis to assess areal and scale dependence of upland landscape structures. Poster paper presented at Remote Sensing and Photogrammetric Society (RSPSoc) annual conference, Aberdeen, 7-10 September 2004.

Liddaman LC. 2004 The use of pattern analysis to assess the scale dependence of upland landscape structures in eroding blanket peat. Remote Sensing and Photogrammetric Society (RSPSoc) Student meeting, Edinburgh, 1-2 April 2004.

Lillesand TM, Kiefer RW and Chipman JW. 2003. Remote Sensing and Image Interpretation, New York: Wiley International: 5th edition

Lindsay JB. 2005. The Terrain Analysis System: A tool for hydro-geomorphic applications. Hydrological Processes, 19(5): 1123-1130.

Lindsay JB. 2006. Sensitivity of channel mapping techniques to uncertainty in digital elevation data. International Journal of Geographical Information Science, 20(6): 669-692.

Lindsay JB and Evans MG. 2006. Using elevation residual analysis for mapping peatland gully networks from LiDAR data. The International Symposium on Terrain Analysis and Digital Terrain Modelling. November 23-25, Nanjing China.

Lindsay JB, Liddaman L, Evans MG and McMorrow J. 2006. Swapping subcatchments for isobasins. Proceedings of the GIS Research UK 14th Annual Conference, pp. 29-33.

Mather (2004) Computer Processing of Remotely Sensed Images: an introduction, Wiley, Chichester, 3rd edition, 324pp.

McGarigal K and BJ Marks. 1995. FRAGSTATS: spatial pattern analysis program for quantifying landscape structure. Gen. Tech. Report PNW-GTR-351, USDA Forest Service, Pacific Northwest Research Station, Portland, OR.

McMorrow JM and Hume E. 1986. Problems of applying multispectral classification to upland vegetation. International Archives of Photogrammetry and Remote Sensing, 26: 610-620.

McMorrow J, Aylen J, Albertson K, Cavan, G, Lindley S, Handley J and Karooni R. 2006. Moorland Wildfires in the Peak District National Park. Climate Change and the Visitor Economy (CCVE) Technical Report 3.[available online, last accessed 8 June 2006] http://www.snw.org.uk/tourism/down_research.html

Mehner H, Cutler M, Fairbairn D and Thompson G. 2004. Remote sensing of upland vegetation: the potential of high spatial resolution satellite sensors. Global Ecology and Biogeography 13 (4): 359–369.

Moors for the Future. 2005. Data booklet. [available online, accessed 28 July 2006] http://www.moorsforthefuture.org.uk/mftf/downloads/publications/Data%20Booklet.pdf

Morton AJ. 1986. Moorland plant community recognition using Landsat MSS data. Remote Sensing of Environment, 20: 291-298.

Pal, M and Mather PM. 2005. Support vector machines for classification in remote sensing. International Journal of Remote Sensing 26 (5): 1007-1011.

Palylyk, CL and Crown, PH. 1984. Application of clustering of Landsat MSS digital data for peatland inventory. *Canadian Journal of Remote Sensing,* 10: 201-208.

Poulin M, Careau D, Rochefort L and Evans M. 2002. From satellite imagery to peatland vegetation diversity: how reliable are habitat maps? *Conservation Ecology*, 6 (2): 16.

NERC ARSF. 2006, Natural Environment Research Council, Airborne Remote Survey Facility. The ARSF instrument suite. http://arsf.nerc.ac.uk/instruments/ [available online, accessed 26 July 2006]

Richards JA. 1995. Remote Sensing Digital Image Analysis: an introduction. Springer-Verlag.

Stewart JM and Wheatly RE. 1990. Estimates of CO_2 production from eroding peat surfaces. Soil Biology and Biochemistry, 22: 65-68.

Ward SA and Weaver RE. 1989. Monitoring heather burning in the North Yorks Moors National Park using multi temporal Thematic Mapper data. International Journal of Remote Sensing, 10 (7): 1151-1153.

Weaver RE. 1987. Spectral separation of moorland vegetation in airborne Thematic Mapper data. International Journal of Remote Sensing, 8 (1): 34-55.

Worrall F, Reed M and Warburton J. 2003 Carbon budget for a British upland peat catchment - Science of the Total Environment, 312 (1-3): 133-146.